



저작자표시-비영리-변경금지 2.0 대한민국

이용자는 아래의 조건을 따르는 경우에 한하여 자유롭게

- 이 저작물을 복제, 배포, 전송, 전시, 공연 및 방송할 수 있습니다.

다음과 같은 조건을 따라야 합니다:



저작자표시. 귀하는 원저작자를 표시하여야 합니다.



비영리. 귀하는 이 저작물을 영리 목적으로 이용할 수 없습니다.



변경금지. 귀하는 이 저작물을 개작, 변형 또는 가공할 수 없습니다.

- 귀하는, 이 저작물의 재이용이나 배포의 경우, 이 저작물에 적용된 이용허락조건을 명확하게 나타내어야 합니다.
- 저작권자로부터 별도의 허가를 받으면 이러한 조건들은 적용되지 않습니다.

저작권법에 따른 이용자의 권리는 위의 내용에 의하여 영향을 받지 않습니다.

이것은 [이용허락규약\(Legal Code\)](#)을 이해하기 쉽게 요약한 것입니다.

[Disclaimer](#)

이학박사학위논문

Loss-tolerant teleportation using hybrid entanglement of light

빛의 이중 양자 얽힘을 통한 손실에 강한
양자공간이동

2021년 2월

서울대학교 대학원
물리천문학부
최성전

Loss-tolerant teleportation using hybrid entanglement of light

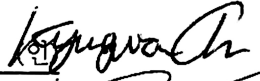




빛의 이중 양자 얽힘을 통한 손실에 강한
양자공간이동

지도교수 정현석

이 논문을 이학박사 학위논문으로 제출함
2020년 12월

서울대학교 대학원
물리천문학부
최성전

최성전의 박사 학위논문을 인준함
2021년 1월

위원장	안경원	
부위원장	정현석	
위원	김석	(인) 
위원	박철환	(인) 
위원	이승우	(인) 

Loss-tolerant teleportation using hybrid entanglement of light

Seongjeon Choi

Supervised by

Professor **Hyunseok Jeong**

A Dissertation

Submitted to the Faculty of

Seoul National University

in Partial Fulfillment of

the Requirements for the Degree of

Doctor of Philosophy

February 2021

Department of Physics and Astronomy

The Graduate School

Seoul National University

Abstract

Loss-tolerant teleportation using hybrid entanglement of light

Seongjeon Choi

Department of Physics and Astronomy

The Graduate School

Seoul National University

The optical system is one of the promising candidates for quantum information processing. Using quantum resources possible for the optical state, one can gain quantum advantages in many useful applications. Quantum teleportation is one of the outstanding protocols using entanglement. However, the unavoidable photon loss damages the entanglement, especially for the optical qubit having many photons.

This dissertation discusses the usage of the hybrid entanglement between two different qubit encodings to achieve both the high teleportation success probability and the high fidelity between the input and target qubit. For the high success probability, I utilize the many-photon qubit encoding such as the coherent-state qubit with large amplitude and multiphoton qubit of polarized photons since these encodings have the nearly-deterministic Bell-state measurement schemes. The small-photon qubit encoding, in contrast, shows the better behavior on the photon loss. This encoding includes

a vacuum-and-single-photon (VSP) qubit, polarized single-photon (PSP) qubit, and coherent-state qubit with a small amplitude. I consider the hybrid entanglement for a coherent-state qubit to a VSP qubit and a multiphoton qubit to all small-photon qubits.

First, the analysis of the hybrid entanglement of a coherent-state qubit shows that the success probability withstands more photon losses as the amplitude of coherent-state qubit increases. The fidelity is affected by the losses both on the coherent-state qubit and VSP qubit, but the loss of the coherent-state qubit affects it more severely especially for large amplitude. Second, the hybrid entanglement of a multiphoton qubit shows that the fidelity is determined by the loss of the small-photon qubit side while the success probability depends on loss only in the multiphoton qubit side. Especially, the hybrid entanglement with the VSP qubit tolerates 10 times more photon-loss rate than the direct transmission in high fidelity regime ($F \geq 90\%$). For the success probability, I propose the optimal photon number consisting of a multiphoton qubit. The generation methods for the required entangled states are additionally discussed.

I further investigate the quantum resources of light other than entanglement: coherence and nonclassicality. I propose physically motivated coherence measures from the role of coherence in the quantum Fisher information and expectation values of quantum observables. For the latter measure, the semidefinite programming provides an efficient method to compute the involved optimization. The suggested nonclassicality measure is based on the negativity of the Glauber-Sudarshan P function. The singular behavior of the P function is dealt with by the filtering on the Fourier space. The nega-

tivity is proven to be equivalent to the robustness of mixing with the classical state, which gives its operational meaning.

Keywords : Teleportation, Hybrid entanglement, Quantum coherence, Non-classicality

Student Number : 2015-20354

Contents

Abstract	i
I. Introduction	1
II. Hybrid entanglement of light and teleportation of many-photon qubit encodings	5
2.1 Introduction	5
2.2 Photon-loss model	7
2.3 Teleportation using the hybrid entanglement between a VSP qubit and a coherent-state qubit	8
2.3.1 Loss on hybrid entanglement	8
2.3.2 Output state of the teleportation	9
2.3.3 Fidelity	12
2.3.4 Success probability	13
2.4 Teleportation of a multi-photon qubit using a carrier qubit . .	15
2.4.1 Review of multiphoton qubit	15
2.4.2 Loss on hybrid entangled states	17
2.4.3 Output states and their fidelities	22
2.4.4 Success probabilities	31
2.5 Generation of hybrid entangled states	34
2.6 Remarks	38
III. Operational quantum resources beyond entanglement	43

3.1	Introduction	43
3.2	Measuring coherence via observable quantum effects	45
3.2.1	Preliminaries	45
3.2.2	Coherence and Quantum Fisher Information	47
3.2.3	Coherence measures from quantum observables	54
3.2.4	Examples	63
3.3	Measuring Nonclassicality via negativity	65
3.3.1	Nonclassicality filtering	65
3.3.2	Negativity as a linear optical monotone	70
3.3.3	Operational interpretations of the negativity	72
3.3.4	Approximate nonclassicality monotones	75
3.3.5	Examples	79
3.4	Remarks	81
IV.	Conclusion	85
	Bibliography	89
	Abstract in Korean	103

List of Figures

<p>Figure 1. Contour graph of the average fidelities of teleportation of $c \rightarrow s$ as a function of the loss rate on the coherent-state qubit side η_c and the VSP qubit side η_s for $\alpha ^2 = 1, 2$, and 3.</p>	13
<p>Figure 2. Success probabilities for teleportation from a coherent-state qubit to a single-rail qubit ($c \rightarrow s$) with several photon numbers ($\alpha ^2 = 1, 2, 3, 4$) against the photon-loss rate on the coherent-state qubit side η_c.</p>	14
<p>Figure 3. Degrees of entanglement (negativity) against the photon-loss rate for the multiphoton qubit $\eta_M = 1 - t_M^2$ and for the carrier qubit $\eta_C = 1 - t_C^2$ of hybrid entanglement between (a) the multiphoton qubit and the coherent-state qubit ρ_{mc}, (b) the multiphoton qubit and the PSP qubit ρ_{mp}, and the multiphoton qubit and the VSP qubit ρ_{ms}. The number of photons N for the multiphoton qubit is set to be $N = 4$. The amplitude of the coherent-state qubit is chosen to be $\alpha = 1.2$.</p>	21

Figure 4.	Schematic of the Bell-state measurement for multiphoton-qubit encoding using beam splitters (BSs), Half-wave plates (HWPs), and on-off photodetectors (PDs). Two on-off photodetectors and one polarizing beam splitter (PBS) are used to measure the polarization of a single photon. The mode labels $1, 2, \dots, N$ ($1', 2', \dots, N'$) represent the corresponding modes of the first (second) multiphoton qubit.	22
Figure 5.	Average fidelities of direct transmission with $N = 4$ (black solid) and hybrid architectures with different carrier qubits: coherent state qubits (denoted by c) for $\alpha = 1.2$ (yellow dot-dashed) and $\alpha = 1.6$ (red dot-dot-dashed), a PSP qubit (p, green dashed), and a VSP qubit (s, blue dotted) against the photon-lose rate for the carrier-qubit part $\eta_C = 1 - t_C^2$. The gray horizontal dotted line is the classical limit $F_{cl} = 2/3$	28
Figure 6.	Success probability P_{success} of the multiphoton Bell-state measurement against the photon-loss rate for the multiphoton qubit $\eta_M = 1 - t_M^2$ for photon numbers of $N = 1, 2, 3$, and 4.	32
Figure 7.	Conceptual schematics for (a) generating hybrid entangled state between a coherent-state qubit and VSP qubit and implementing conversion gates (b) $V_{p \rightarrow s}$ and (c) $V_{p \rightarrow c}$	42

Figure 8. Comparisons between the lower bounds of the super-radiant based measure C_S (red, \circ), the QFI based measure C_F^M (green, \square), and the relative entropy of coherence C_R (blue, \times) for the M -qubit Dicke state with k excitations $|M, k\rangle$. The plots are normalized so they coincide at $k = 10$, and demonstrate qualitatively similar behaviour across different measures. 64

Figure 9. Comparisons among the l_1 norm of coherence C_{l_1} (green, solid), the relative entropy of coherence C_D (red, dash-dotted), and the coherence measure corresponding to magnetization measurement C_{S_x} (blue, dotted). I consider the single parameter, 3 qubit state $\rho = (1 + p/7)\mathbb{1}/8 - p/7|w\rangle\langle w|$, where $|w\rangle := \frac{1}{\sqrt{3}}(|001\rangle + |010\rangle + |100\rangle)$ and $p \in [0, 1]$ 66

Figure 10. (a) Convergence of the filtered negativity(solid line) $\mathcal{N}_{\Omega, w}$ to the negativity(dotted line) \mathcal{N} for the single photon added thermal state ρ_{SPAT} with $\bar{n} = 2$. (b) The (logged) filtered negativity $\log(1 + \mathcal{N}_{\Omega, w})$ for squeezed vacuum $|r\rangle$ 80

List of Tables

Table 1. Maximum photon-loss rates for the carrier qubit, η_C , required to reach the fidelity of 99.9%, 99%, and 90% with the coherent-state (CS) qubit, the PSP qubit, and the VSP qubit. The direct transmission (DT) of the multiphoton qubit with the photon number $N = 4$ is given for comparison under the same photon-loss rate.	31
--	----

Chapter 1

Introduction

The revolutionary development of quantum optics in the late 20th century allows physicists to prepare and control an individual quantum system. Beyond passively observing quantum effects, the engineering ability on the quantum system opens up the quantum technology that takes advantage of the characteristics of quantum mechanics. The contemporary discoveries of the fundamental protocols, therefore, do not seem just coincidences: C. H. Bennett and G. Brassard invented the radically innovative secret-key sharing protocol [1]. Shor's algorithm [2] and Grover's algorithm [3] became fundamental for the quantum algorithms. Braunstein and Caves gave the idea of quantum metrology [4].

Quantum teleportation is one of the distinctive protocols in quantum information processing. Discovered by C. H. Bennett, G. Brassard, and C. Crepeau [5], teleportation indirectly transfers quantum information without the information itself moving through physical space. This striking feature has no imitation in the classical information theory. Although the information is transferred only after enough amount of classical information is transmitted despite its seemingly 'non-local' appearance, teleportation has useful applications in quantum communication [6, 7] and quantum computing [8, 9, 10].

One of the main obstacles of optical quantum information is the in-

evitable decoherence due to photon loss. Especially for long-distance quantum information processing, it is highly desirable to find teleportation protocols loss-tolerant under the photon loss. There has been suggested such as purification protocol [11, 12], entanglement swapping with quantum repeaters [13], and error-correcting protocol [14, 15, 16, 17] in repeater nodes. Additionally, the study on the robust qubit encodings and their hybrid has been introduced. This dissertation particularly focuses on the hybrid approach aiming to combine the merits of different qubit encodings. This approach is believed to be possible in the near future.

For teleportation, a special kind of correlation, entanglement, must be shared between the sender and receiver, which the classical mechanics cannot provide. The entanglement, however, is not the only distinctive feature in the optical system: there are other quantum characteristics of optical system [18, 19, 20, 21]. The famous particle-wave duality of light tells that the light is not particle nor wave: the quantum nature of light has both of them [22]. In other words, if an optical state is solely described by the particles or waves without superposition, the system is classical and cannot show the quantum power. The resource theory framework provides the quantitative understanding of the quantumness in the perspective of each characteristic. The degree of deviation from the classical particle and wave description is called quantum coherence and nonclassicality, respectively. The central issue of the resource theory framework is to find operational measures. The *operational* measure does not merely quantify, but the measured quantity itself has a physical implication in some operational scenario.

In this dissertation, the usage of the hybrid entanglement is discussed

for loss-robust qubit teleportation and investigate the operational measures that may quantify the coherence and nonclassicality. In chapter 2, I consider the hybrid entanglement between a many-photon qubit and a small-photon qubit. The former has merit on the Bell-state measurement, and the latter on the loss-tolerance. In chapter 3, I introduce the resource-theoretic measures for coherence and nonclassicality. I drive the coherence measures from the famous quantum effects such as metrological power and expectation values of quantum observables. For the nonclassicality, I show that the famous phase-space negativity can be a genuine measure and that it is equivalent to the robustness of the mixing with classical states.

Chapter 2

Hybrid entanglement of light and teleportation of many-photon qubit encodings

2.1 Introduction

Photonic qubits are particularly useful for quantum information transfer over a long distance. There are several different ways to encode qubit information in traveling light fields. Probably the most well-known type uses the horizontal and vertical polarizations of a single photon (PSP), $|H\rangle$ and $|V\rangle$ [8, 23], which is often called “dual-rail encoding.” Another method is to utilize the vacuum and the single-photon (VSP) states, $|0\rangle$ and $|1\rangle$, called “single-rail encoding,” with its own merit [24, 25]. Recently, Lee *et al.* suggested multiphoton encoding with the horizontal and vertical polarizations of N photons, $\{|H\rangle^{\otimes N} = \bigotimes_{i=1}^N |H\rangle_i, |V\rangle^{\otimes N} = \bigotimes_{i=1}^N |V\rangle_i\}$. Not only restricted to the discrete qubit encoding, one can alternatively utilize continuous-variable-based qubit encoding such as one with two coherent states with opposite phases, $|\pm\alpha\rangle$, where $\pm\alpha$ are coherent amplitudes [26, 27]. The characteristic of the coherent-state qubit is subject to the amplitude α .

The aforementioned qubit encodings can be divided into two groups

according to the mean-photon number \bar{n} . The first one is the small-photon qubit encoding, which includes the PSP qubit, VSP qubit, and the coherent-state qubit with a small α . The mean photon numbers in these encodings are less than two. With the linear optics, only two among four Bell states can be discriminated for the PSP qubit and VSP qubit, so the success probability of Bell measurement is generally limited to $1/2$ [28, 29]. The success probability of the coherent-state qubit is also small since it is given by $1 - O(e^{-2\alpha^2})$ [26]. This affects the success probabilities of gate operations for linear optics quantum computing [8] depending on the gate teleportation scheme [10], which is an obstacle against the implementation of scalable optical quantum computation.

The second group contains the multiphoton qubit and the coherent-state qubit with a large α . In contrast to the first one, these qubits have the nearly-deterministic Bell-state measurement scheme approaching the unity as $\bar{n} \rightarrow \infty$. However, the many-photon qubits are fragile under the photon loss since these qubits generally form macroscopic superposition, which is weak under loss.

These two groups have their own merits. The hybrid approach aims to combine the advantages of qubit encodings and redeem the weaknesses. In this chapter, I consider the hybrid entanglement of small-photon and many-photon qubits and investigate teleportation schemes via the hybrid entanglement. The evaluation of this approach will be evaluated by the fidelity between the input and output states and the success probability of quantum teleportation under photon loss. This study may be useful for designing and building up loss-tolerant quantum communication networks.

2.2 Photon-loss model

In this chapter, the photon-loss environment is described by the master equation under the Born-Markov approximation with the zero-temperature [30]:

$$\frac{\partial \rho}{\partial \tau} = \gamma \sum_{i=1}^N \left(\hat{a}_i \rho \hat{a}_i^\dagger - \frac{1}{2} \hat{a}_i^\dagger \hat{a}_i \rho - \frac{1}{2} \rho \hat{a}_i^\dagger \hat{a}_i \right) \quad (2.1)$$

where $\hat{a}_i(\hat{a}_i^\dagger)$ represents the annihilation (creation) operator of mode i and γ is the decay constant determined by the coupling strength of the system and the environment. This evolution is equivalently described by the beam-splitter model where each input mode is mixed with the vacuum state at a beam splitter with transmittance $t = e^{-\gamma\tau/2}$ and reflectance $r = \sqrt{1-t^2}$ [31] and in the Heisenberg picture, the beamsplitter is depicted as

$$\begin{pmatrix} \hat{a} \\ \hat{b} \end{pmatrix} \rightarrow \begin{pmatrix} \hat{a}' \\ \hat{b}' \end{pmatrix} = \begin{pmatrix} t & -r \\ r & t \end{pmatrix} \begin{pmatrix} \hat{a} \\ \hat{b} \end{pmatrix}. \quad (2.2)$$

where $\hat{a}(\hat{b})$ is the annihilation operator on system (ancillary) mode. The output state is then obtained by tracing out the ancillary modes. Since the evolution of a single photon state is given by $|1\rangle\langle 1| \rightarrow t^2 |1\rangle\langle 1| + r^2 |0\rangle\langle 0|$, I call the square of the reflectance r^2 the photon-loss rate η .

Under the photon loss, each qubit has its noise behavior according to its physical realization. For instance, a VSP qubit basis consists of a vacuum state $|0\rangle$ and a single-photon state $|1\rangle$. The vacuum does not change under loss and the single-photon decays to the vacuum. The loss on the coherent-

state qubit, in contrast, induces dephasing and amplitude damping. The loss of the hybrid entangled states is shown in the mixture of both noise behaviors.

2.3 Teleportation using the hybrid entanglement between a VSP qubit and a coherent-state qubit

2.3.1 Loss on hybrid entanglement

Let me consider a hybrid entangled state of a single-rail qubit and a coherent state qubit:

$$|\Psi\rangle_{sc} = \frac{1}{\sqrt{2}} (|0\rangle_s |\alpha\rangle_c + |1\rangle_s |-\alpha\rangle_c), \quad (2.3)$$

where $|\pm\alpha\rangle$ are coherent states of amplitudes $\pm\alpha$. Here, the subscripts s and c stand for the VSP qubit and the coherent-state qubit, respectively, and $\pm\alpha$ are assumed to be real without loss of generality. Note that this type of entanglement was experimentally demonstrated [32].

The effect of the photon loss in Eq. (2.2) on the initial hybrid channel $|\Psi\rangle_{sc}$ leads to the following evolution:

$$\begin{aligned} \rho_{sc}(\alpha; t) = & \frac{1}{2} \left(|0\rangle_s \langle 0| \otimes |t_c \alpha\rangle_c \langle t_c \alpha| + \{ t_s^2 |1\rangle_s \langle 1| + (1 - t_s^2) |0\rangle_s \langle 0| \} \right. \\ & \left. \otimes | -t_c \alpha\rangle_c \langle -t_c \alpha| + t e^{-2\alpha^2(1-t_c^2)} \{ |0\rangle_s \langle 1| \otimes |t_c \alpha\rangle_c \langle -t_c \alpha| + \text{H.c.} \} \right), \end{aligned} \quad (2.4)$$

where t_s and t_c correspond to the transmittance of the beamsplitter model for the VSP and coherent-state qubit part, respectively, which is related to the photon-loss rate as $\eta = 1 - t^2$. Here, I assume the asymmetric environment, i.e. the photon-loss rates on the VSP qubit and coherent-state qubit can be different. The basic scheme is to keep the coherent-state qubit from photon loss at the cost of the loss on the VSP qubit. The justification follows in subsequent sections.

2.3.2 Output state of the teleportation

Now, consider the case where the input qubit is a coherent state qubit in the form of

$$|\psi_{\text{in}}\rangle = \mathcal{N}(a|t_c\alpha\rangle_c + b|-t_c\alpha\rangle_c), \quad (2.5)$$

where $\mathcal{N} = \left\{1 + e^{-2t_c^2\alpha^2}(ab^* + a^*b)\right\}^{-1/2}$, and the target state is a VSP qubit as $|\psi_t\rangle = a|0\rangle_s + b|1\rangle_s$. I use the notation $c \rightarrow s$ for the teleportation from coherent-state qubit to a VSP qubit.

To perform quantum teleportation, the sender needs to perform a Bell-state measurement and the receiver should carry out single-qubit transforms based on the outcome of the Bell-state measurement. In this case, the sender should perform the Bell-state measurement of the coherent-state qubit encoding described below. To reflect feasible conditions, I assume that available resources in addition to hybrid entanglement are passive linear optical elements and photon detection.

The Bell-state measurement for coherent state qubits can be performed

by using a 50:50 beam splitter and two photon-number parity measurements [26]. The four Bell states in the dynamic coherent state basis are

$$\begin{aligned} |\mathcal{B}_{1,2}\rangle_{cc'} &= \mathcal{N}_{\pm} (|t\alpha\rangle_c |t\alpha\rangle_{c'} \pm |-t\alpha\rangle_c |-t\alpha\rangle_{c'}), \\ |\mathcal{B}_{3,4}\rangle_{cc'} &= \mathcal{N}_{\pm} (|t\alpha\rangle_c |-t\alpha\rangle_{c'} \pm |-t\alpha\rangle_c |t\alpha\rangle_{c'}), \end{aligned} \quad (2.6)$$

where $\mathcal{N}_{\pm} = (2 \pm 2 \exp(-4t^2\alpha^2))^{-1/2}$ are normalization factors. The Bell states evolve through the 50:50 beam splitter as

$$\begin{aligned} |\mathcal{B}_1\rangle_{cc'} &\rightarrow \mathcal{N}_+ |even\rangle_c |0\rangle_{c'}, & |\mathcal{B}_2\rangle_{cc'} &\rightarrow \mathcal{N}_- |odd\rangle_c |0\rangle_{c'}, \\ |\mathcal{B}_3\rangle_{cc'} &\rightarrow \mathcal{N}_+ |0\rangle_c |even\rangle_{c'}, & |\mathcal{B}_4\rangle_{cc'} &\rightarrow \mathcal{N}_- |0\rangle_c |odd\rangle_{c'}, \end{aligned} \quad (2.7)$$

where $|even\rangle = |\sqrt{2}t\alpha\rangle + |-\sqrt{2}t\alpha\rangle$ has nonzero photon-number probabilities only for even numbers of photons and $|odd\rangle = |\sqrt{2}t\alpha\rangle - |-\sqrt{2}t\alpha\rangle$ has only for odd numbers of photons. The parity measurement projection operators O_j ,

$$\begin{aligned} \hat{O}_1 &= \sum_{n=1}^{\infty} |2n\rangle_c \langle 2n| \otimes |0\rangle_{c'} \langle 0|, \\ \hat{O}_2 &= \sum_{n=1}^{\infty} |2n-1\rangle_c \langle 2n-1| \otimes |0\rangle_{c'} \langle 0|, \\ \hat{O}_3 &= \sum_{n=1}^{\infty} |0\rangle_c \langle 0| \otimes |2n\rangle_{c'} \langle 2n|, \\ \hat{O}_4 &= \sum_{n=1}^{\infty} |0\rangle_c \langle 0| \otimes |2n-1\rangle_{c'} \langle 2n-1|, \end{aligned} \quad (2.8)$$

where subscript j corresponds to the j -th Bell state, can be used to dis-

criminate between the four states. It should be noted that there is a nonzero probability of getting $|0\rangle_c |0\rangle_{c'}$ for which neither of the detectors registers any photon. Such a case is regarded as a failure event, and the failure probability is $P_f = \exp[-2t^2\alpha^2]$ [26, 33]. The failure event is further discussed in the context of the success probability of the teleportation process later in this section.

According to the standard teleportation protocol, when $|\mathcal{B}_1\rangle_{cc'}$ is measured, no additional operation is required. The output state with the normalization factor is

$$\begin{aligned}\rho_{out}^{c \rightarrow s} &= \frac{\text{Tr}_{cc'} \left\{ (\hat{O}_1)_{cc'} (\hat{U}_{BS})_{cc'} [\rho_{sc'}(\alpha; t) \otimes |\psi\rangle_c \langle \psi|] (\hat{U}_{BS}^\dagger) \right\}}{\text{Tr} \left\{ (\hat{O}_1)_{cc'} (\hat{U}_{BS})_{cc'} [\rho_{sc'}(\alpha; t) \otimes |\psi\rangle_c \langle \psi|] (\hat{U}_{BS}^\dagger) \right\}} \\ &= (|a|^2 + (1-t_s^2)|b|^2) |0\rangle \langle 0| + t_s^2 |b|^2 |1\rangle \langle 1| \\ &\quad + t_s e^{-2\alpha^2(1-t_c^2)} (ab^* |0\rangle \langle 1| + a^* b |1\rangle \langle 0|),\end{aligned}\tag{2.9}$$

where \hat{U}_{BS} represents the 50:50 beam splitter operator defined as $U_{BS} = \exp \left[\frac{\pi}{4} (\hat{a}_0^\dagger \hat{a}_1 - \hat{a}_1 \hat{a}_0^\dagger) \right]$. If $|\mathcal{B}_2\rangle_{cc'}$ is measured, the Pauli-Z operation for the VSP qubit is required to recover the input state, which can be performed by a π -phase shifter. When $|\mathcal{B}_3\rangle_{cc'}$ and $|\mathcal{B}_4\rangle_{cc'}$ are measured, the Pauli-X operation is needed to implement the bit flip, $|0\rangle \leftrightarrow |1\rangle$, which is difficult to realize using linear optics which reserves the photon number. However, the quantum information, stored in two coefficients a and b , is still transmitted and the receiver knows how the input state is changed that can be recovered by the classical post-processing after measurements.

2.3.3 Fidelity

The teleportation process may be evaluated by the fidelity between the input and the output state. Since using the hybrid entanglement changes the qubit encoding, the target state is set to be the ideal output state $|\Psi_t\rangle_s = a|0\rangle_s + a|1\rangle_s$. For the output state in Eq. (2.9), the fidelity is given by

$$\begin{aligned} F_{c \rightarrow s} &= {}_s \langle \Psi_t | \rho_{\text{out}}^{c \rightarrow s} | \Psi_t \rangle_s \\ &= |a|^4 + \left((1 - t_s^2) + 2t_s e^{-2\alpha^2(1-t_c^2)} \right) |a|^2 |b|^2 + t_s^2 |b|^4. \end{aligned}$$

I average the fidelity over all possible input states. It can be found by parametrizing the coefficients of the input state as $a = \cos[\theta/2] \exp[i\phi/2]$ and $b = \sin[\theta/2] \exp[-i\phi/2]$, where $0 \leq \theta < \pi$ and $0 \leq \phi < 2\pi$. Therefore, the analytic form of the average fidelity $F_{c \rightarrow s}^{\text{ave}}$ is

$$\begin{aligned} F_{c \rightarrow s}^{\text{ave}} &= \frac{1}{4\pi} \int_0^\pi d\theta \sin\theta \int_0^{2\pi} d\phi F_{s \rightarrow c} \\ &= \frac{1}{2} + \frac{t_s^2}{6} + \frac{t_s e^{-2\alpha^2(1-t_c^2)}}{3}. \end{aligned} \quad (2.10)$$

The average fidelity shows that, in the limit of the perfect loss on the VSP qubit, $t_s \rightarrow 0$ and $t_c = 1$, the fidelity is bounded by $1/2$ since the output VSP qubit decay to the vacuum $|0\rangle$, regardless of the input. On the other hand, when $t_s = 1$ and $t_c \rightarrow 0$ with large α , the average fidelity is bounded by $2/3$ which is the classical limit without entanglement. Note that the phase information, ab^* and a^*b , is dephased exponentially on the loss of the coherent-state qubit, $\eta_c = 1 - t_c^2$, while it depends on the square root of

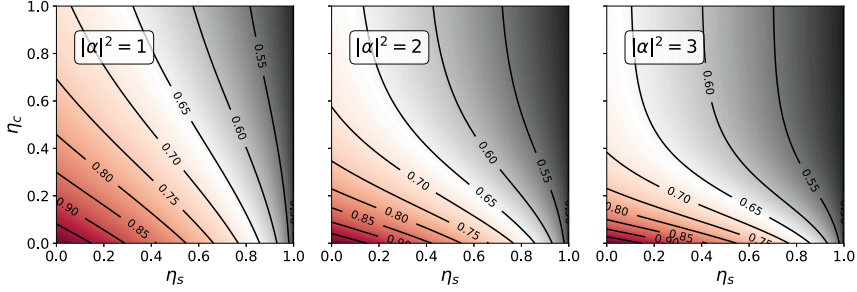


Figure 1: Contour graph of the average fidelities of teleportation of $c \rightarrow s$ as a function of the loss rate on the coherent-state qubit side η_c and the VSP qubit side η_s for $|\alpha|^2 = 1, 2$, and 3.

the loss on the VSP qubit, $\eta_s = 1 - t_s^2$.

In Fig. 1, I present the contour graph of the average fidelity in Eq. 2.10. The graph shows the dependence on the loss rate η_c is severe for large α . When the coherent-state qubit is in the single-photon region $\alpha \sim 1$, the fidelity depends similarly on η_c and η_s . In the many-photon qubit region, however, η_c affects the fidelity more severely than η_s . As mentioned before, this is due to the dephasing induced by η_c . On the other hand, the dependence on η_s remains nearly constant for the small η_c region. This asserts that the hybrid approach is needed for the loss-tolerant transfer of the quantum information of the coherent-state qubit.

2.3.4 Success probability

Now, I analyze the success probability of the teleportation, $P_{c \rightarrow s}$, which is strongly related to the success probability of the Bell-state measurement. The Bell-state measurement for coherent state qubits can identify all four Bell states with the success probability of $1 - e^{-2r_c^2 \alpha^2}$ [26, 33]. I pointed out

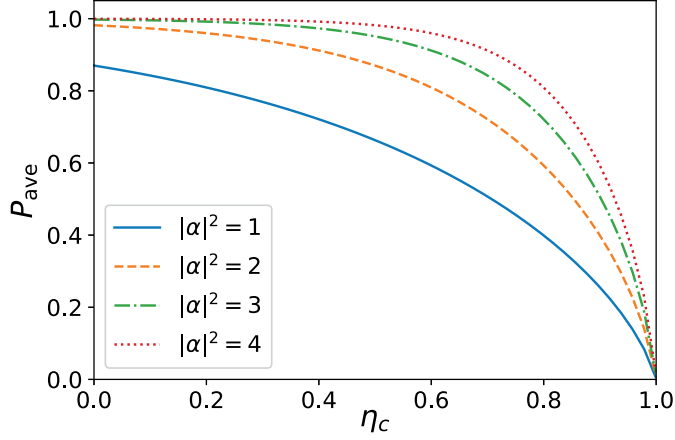


Figure 2: Success probabilities for teleportation from a coherent-state qubit to a single-rail qubit ($c \rightarrow s$) with several photon numbers ($|\alpha|^2 = 1, 2, 3, 4$) against the photon-loss rate on the coherent-state qubit side η_c .

that a local single-qubit operation, the Pauli-X operation which flips $|0\rangle$ and $|1\rangle$, cannot be effectively performed using linear optics elements. However, this case can be seen as a success since the quantum information in the input state is still transferred.

The success probability of the teleportation is obtained by

$$P_{c \rightarrow s} = \sum_i \left\langle U_{\text{BS}}^\dagger \hat{O}_i U_{\text{BS}} \right\rangle = \frac{1 - e^{-2t_c^2 \alpha^2}}{1 + e^{-2t_c^2 \alpha^2} (ab^* + a^*b)}. \quad (2.11)$$

The numerator comes from the normalization factor of the input state given by the coherent-state qubit. This shows that the success probability does not depend on the photon loss on the VSP qubit. The average success probability of the teleportation can be similarly obtained like Eq. (2.10). Figure 2 shows the average success probability obtained by the numerical integration. Note that the teleportation is nearly deterministic when the amplitude

of the coherent-state is large. Moreover, the region that the success probability is nearly 1 also becomes broad. This shows that the hybrid with the coherent-state qubit has merits on the teleportation success probability even under loss.

2.4 Teleportation of a multi-photon qubit using a carrier qubit

In this section, I investigate teleportation using a hybrid entangled state between a multiphoton qubit and a small-photon qubit for the loss-tolerant transfer of the quantum information in a multiphoton qubit. In what follows, the small-photon qubit is also called the carrier qubit to stress the usage of them for information carriers.

2.4.1 Review of multiphoton qubit

The multiphoton qubit is suggested by Lee. *et al.* [34, 35] mainly for the Bell-state measurement. I first review the basic properties of the multiphoton encoding for quantum computation. I temporarily denote the multiphoton qubit as $|0_L\rangle := |H\rangle^{\otimes N}$ and $|1_L\rangle := |V\rangle^{\otimes N}$ only in this subsection. To realize universal quantum computation, one needs to implement a set of quantum operations, known as the universal gate set. It contains Pauli X gate, arbitrary phase rotations, Hadamard gate, and CNOT gate.

Pauli X gate and phase rotations are easy to implement for the multiphoton qubit. Applying the polarization rotator: $\{|H\rangle, |V\rangle\} \rightarrow \{|V\rangle, |H\rangle\}$ on each mode, we can do Pauli X gate. A phase rotation with an arbitrary

trary phase θ can be implemented by applying a phase-shifter $\{|H\rangle, |V\rangle\} \rightarrow \{|H\rangle, e^{i\theta}|V\rangle\}$ on one of N modes.

The implementation of the Hardamard gate and CNOT gate can be accomplished by utilizing the teleportation. Teleportation with an entangled state $|H\rangle \propto |0_L\rangle|+_L\rangle + |1_L\rangle|-_L\rangle$ and a feed-forward yields the Hardamard gate on the input qubit. Similarly, the CNOT gate can be implemented with an entangled state

$$|0_L 0_L\rangle|0_L 0_L\rangle + |0_L 1_L\rangle|0_L 1_L\rangle + |1_L 0_L\rangle|1_L 1_L\rangle + |1_L 1_L\rangle|1_L 0_L\rangle.$$

In these cases, the required resources are the entangled states needed for the teleportation.

For photonic qubits, one need to consider the photon loss, which is one of the major error sources. Here, I demonstrate the property of the multiphoton qubit under photon-loss environment. Suppose transmitting a multiphoton qubit of N photons $|\psi_{\text{in}}\rangle = a|H\rangle^{\otimes N} + b|V\rangle^{\otimes N}$ over a lossy environment directly. The output qubit of the transmission is obtained using Eq. (2.2) as

$$\begin{aligned} \rho_{\text{out}}(t) &= |a|^2 [t^2 |H\rangle\langle H| + (1-t^2) |0\rangle\langle 0|]^{\otimes N} + |b|^2 [t^2 |V\rangle\langle V| + (1-t^2) |0\rangle\langle 0|]^{\otimes N} \\ &\quad + t^{2N} [ab^* (|H\rangle\langle V|)^{\otimes N} + \text{H.c.}] \\ &= t^{2N} |\psi_{\text{in}}\rangle\langle\psi_{\text{in}}| + (1-t^{2N}) \rho^{\text{loss}}, \end{aligned}$$

where

$$\begin{aligned} \rho^{\text{loss}} = & \sum_{k=1}^N (t^2)^{N-k} (1-t^2)^k \sum_{\mathcal{P} \in \text{Perm}(N,k)} \left\{ |a|^2 \mathcal{P}[(|H\rangle\langle H|)^{\otimes N-k} \otimes (|0\rangle\langle 0|)^{\otimes k}] \right. \\ & \left. + |b|^2 \mathcal{P}[(|V\rangle\langle V|)^{\otimes N-k} \otimes (|0\rangle\langle 0|)^{\otimes k}] \right\} \end{aligned} \quad (2.12)$$

is the loss term with one or more photons lost. I denote $\text{Perm}(N, k)$ as the set of permutations of tensor products with the number of elements $\binom{N}{k}$, which represents the cases that photons in k modes within the total N modes are lost and photons in $N - k$ modes remain in the polarization state. It is straightforward to see that ρ^{loss} is orthogonal to $|\psi_{\text{in}}\rangle$. The quality of the output state is measured by fidelity F between the input and output states that is defined as $F(t) = \langle \psi_{\text{in}} | \rho_{\text{out}}(t) | \psi_{\text{in}} \rangle$. The fidelity for the direct transmission is then obtained as

$$F^{\text{dir}} = t^{2N} = (1 - \eta)^N.$$

This shows that the multiphoton qubit becomes more fragile when photon number N per qubit becomes larger. Although the success probability of the Bell-state measurement using multiphoton qubits approaches the unity as N gets larger [34], this fragility may be a weak point of the multiphoton encoding when it is applied to quantum information transfer.

2.4.2 Loss on hybrid entangled states

For the teleportation between two different types of qubits, the sender and the receiver need to share a hybrid entangled state between a multipho-

ton qubit and a carrier qubit. The entangled state is expressed as $|\psi_{\text{hyb}}\rangle = \frac{1}{\sqrt{2}}(|H\rangle^{\otimes N}|C_0\rangle + |V\rangle^{\otimes N}|C_1\rangle)$, where $|C_0\rangle$ and $|C_1\rangle$ are the basis states for the carrier qubit. I consider the three types of hybrid entangled states

$$\begin{aligned} |\psi_{\text{mc}}\rangle &= \frac{1}{\sqrt{2}} \left(|H\rangle^{\otimes N} |\alpha\rangle + |V\rangle^{\otimes N} |-\alpha\rangle \right), \\ |\psi_{\text{mp}}\rangle &= \frac{1}{\sqrt{2}} \left(|H\rangle^{\otimes N} |H\rangle + |V\rangle^{\otimes N} |V\rangle \right), \\ |\psi_{\text{ms}}\rangle &= \frac{1}{\sqrt{2}} \left(|H\rangle^{\otimes N} |0\rangle + |V\rangle^{\otimes N} |1\rangle \right), \end{aligned} \quad (2.13)$$

where subscripts m, c, p and s denote multiphoton qubit, coherent-state qubit, PSP qubit, and VSP qubit, respectively.

I assume an asymmetric environment that the transmittance (reflectance) of every mode of the multiphoton qubit is t_M (r_M) and that of the carrier qubit is t_C (r_C). Using Eq. (2.2), the shared hybrid entangled states are obtained as

$$\begin{aligned} \rho_{\text{mc}}(t_M, t_C) &= \frac{t_M^{2N}}{2} \left\{ (|H\rangle\langle H|)^{\otimes N} \otimes |t_C\alpha\rangle\langle t_C\alpha| + (|V\rangle\langle V|)^{\otimes N} \otimes |-t_C\alpha\rangle\langle -t_C\alpha| \right. \\ &\quad \left. + e^{-2\alpha^2 r_C^2} [(|H\rangle\langle V|)^{\otimes N} \otimes |t_C\alpha\rangle\langle -t_C\alpha| + \text{H.c.}] \right\} + (1 - t_M^{2N}) \rho_{\text{mc}}^{\text{loss}}, \end{aligned} \quad (2.14)$$

$$\begin{aligned} \rho_{\text{mp}}(t_M, t_C) &= t_M^{2N} \left\{ t_C^2 |\psi_{\text{mp}}\rangle\langle\psi_{\text{mp}}| + r_C^2 [(|H\rangle\langle H|)^{\otimes N + (|V\rangle\langle V|)^{\otimes N}}] \otimes |0\rangle\langle 0| \right\} \\ &\quad + (1 - t_M^{2N}) \rho_{\text{mp}}^{\text{loss}}, \end{aligned} \quad (2.15)$$

and

$$\begin{aligned} \rho_{\text{ms}}(t_M, t_C) = & \frac{t_M^{2N}}{2} \left\{ (|H\rangle\langle H|)^{\otimes N} \otimes |0\rangle\langle 0| + (|V\rangle\langle V|)^{\otimes N} \otimes (t_C^2 |1\rangle\langle 1| + r_C^2 |0\rangle\langle 0|) \right. \\ & \left. + t_C [(|H\rangle\langle V|)^{\otimes N} \otimes |0\rangle\langle 1| + \text{H.c.}] \right\} + (1 - t_M^{2N}) \rho_{\text{ms}}^{\text{loss}}, \quad (2.16) \end{aligned}$$

where the loss terms ρ^{loss} represent the events where one or more photons are lost from the multiphoton qubit. Explicit expressions of the loss terms are

$$\begin{aligned} \rho_{\text{mc}}^{\text{loss}} = & \frac{1}{2} \sum_{k=1}^N (t_M^2)^{N-k} (1 - t_M^2)^k \sum_{\mathcal{P} \in \text{Perm}(N,k)} \\ & \left\{ \mathcal{P} [(|H\rangle\langle H|)^{\otimes N-k} \otimes (|0\rangle\langle 0|)^{\otimes k}] \otimes |t_C \alpha\rangle\langle t_C \alpha| \right. \\ & \left. + \mathcal{P} [(|V\rangle\langle V|)^{\otimes N-k} \otimes (|0\rangle\langle 0|)^{\otimes k}] \otimes |-t_C \alpha\rangle\langle -t_C \alpha| \right\}, \end{aligned}$$

$$\begin{aligned} \rho_{\text{mp}}^{\text{loss}} = & \frac{1}{2} \sum_{k=1}^N (t_M^2)^{N-k} (1 - t_M^2)^k \sum_{\mathcal{P} \in \text{Perm}(N,k)} \\ & \left\{ \mathcal{P} [(|H\rangle\langle H|)^{\otimes N-k} \otimes (|0\rangle\langle 0|)^{\otimes k}] \otimes (t_C^2 |H\rangle\langle H| + r_C^2 |0\rangle\langle 0|) \right. \\ & \left. + \mathcal{P} [(|V\rangle\langle V|)^{\otimes N-k} \otimes (|0\rangle\langle 0|)^{\otimes k}] \otimes (t_C^2 |V\rangle\langle V| + r_C^2 |0\rangle\langle 0|) \right\}, \end{aligned}$$

and

$$\begin{aligned} \rho_{\text{ms}}^{\text{loss}} = & \frac{1}{2} \sum_{k=1}^N (t_M^2)^{N-k} (1 - t_M^2)^k \sum_{\mathcal{P} \in \text{Perm}(N,k)} \\ & \left\{ \mathcal{P} [(|H\rangle\langle H|)^{\otimes N-k} \otimes (|0\rangle\langle 0|)^{\otimes k}] \otimes (t_C^2 |1\rangle\langle 1| + r_C^2 |0\rangle\langle 0|) \right. \\ & \left. + \mathcal{P} [(|V\rangle\langle V|)^{\otimes N-k} \otimes (|0\rangle\langle 0|)^{\otimes k}] \otimes |0\rangle\langle 0| \right\}. \end{aligned}$$

All these terms do not contain entanglement. This is attributed to the fact that when a photon from the multiphoton qubit is lost, the resulting multiphoton qubit effectively becomes completely dephased.

I now investigate the amount of entanglement contained in the hybrid entangled states. Entanglement in any bipartite mixed state can be measured by the negativity $\mathcal{N}(\rho)$ [36], which is defined as

$$\mathcal{N}(\rho) \equiv \frac{\|\rho^{T_A}\| - 1}{2} = \sum_{\lambda_i < 0} |\lambda_i| \quad (2.17)$$

where ρ^{T_A} is the partial transpose of ρ with respect to subsystem A , $\|\cdot\|$ is the trace norm, and $\{\lambda_i\}$ is the set of eigenvalues of ρ^{T_A} . The negativity is an entanglement measure, i.e., it does not increase under any local operations and classical communications.

Using Eq. (2.17), analytical expressions of the negativity of the hybrid entangled states can be obtained from Eqs. (2.14), (2.15) and (2.16). Although $|t_C\alpha\rangle$ and $|-t_C\alpha\rangle$ in Eq. (2.14) are not orthogonal, they are two linear independent state vectors that can be treated in a two-dimensional Hilbert space as done in Ref. [26]. Further, since the loss terms, ρ^{loss} , are orthogonal to the remaining terms and contain no entanglement, I can consider only the remaining terms in a $2 \otimes 2$ dimensional Hilbert space. The

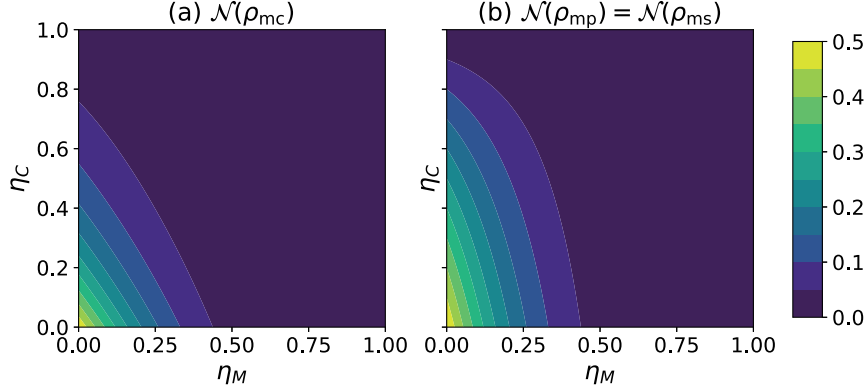


Figure 3: Degrees of entanglement (negativity) against the photon-loss rate for the multiphoton qubit $\eta_M = 1 - t_M^2$ and for the carrier qubit $\eta_C = 1 - t_C^2$ of hybrid entanglement between (a) the multiphoton qubit and the coherent-state qubit ρ_{mc} , (b) the multiphoton qubit and the PSP qubit ρ_{mp} , and the multiphoton qubit and the VSP qubit ρ_{ms} . The number of photons N for the multiphoton qubit is set to be $N = 4$. The amplitude of the coherent-state qubit is chosen to be $\alpha = 1.2$.

degrees of negativity are then obtained as

$$\begin{aligned} \mathcal{N}(\rho_{mc}) &= \frac{t_M^{2N}}{4\sqrt{1 - e^{-4t_C^2\alpha^2}}} \\ &\times \left[\sqrt{1 - 2\left(2e^{-4t_C^2\alpha^2} - 1\right)e^{-2r_C^2\alpha^2} + e^{-4r_C^2\alpha^2}} \right. \\ &\quad \left. + e^{-2r_C^2\alpha^2} - 1 \right], \\ \mathcal{N}(\rho_{mp}) &= \mathcal{N}(\rho_{ms}) = \frac{1}{2}t_M^{2N}t_C^2. \end{aligned}$$

Here, the negativities of ρ_{mp} and ρ_{ms} are same, because entanglement disappears when at least one photon is definitely lost in both cases.

Figure 3 shows the dependence of the negativity on the photon loss rates of both the sides, $\eta_M = 1 - t_M^2$ and $\eta_C = 1 - t_C^2$. It is generally shown

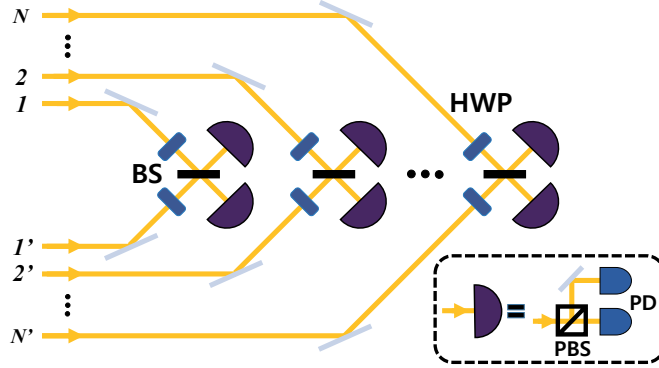


Figure 4: Schematic of the Bell-state measurement for multiphoton-qubit encoding using beam splitters (BSs), Half-wave plates (HWPs), and on-off photodetectors (PDs). Two on-off photodetectors and one polarizing beam splitter (PBS) are used to measure the polarization of a single photon. The mode labels $1, 2, \dots, N$ ($1', 2', \dots, N'$) represent the corresponding modes of the first (second) multiphoton qubit.

that the dependence is sharper for the loss rate, η_M , of the multiphoton qubit than that of the carrier qubit, η_C . This implies the desirable property that entanglement in the hybrid entangled state is more robust to the photon loss on the carrier qubit than that on the multiphoton qubit.

2.4.3 Output states and their fidelities

Let me consider quantum teleportation with the hybrid entangled states ρ_{mc} , ρ_{mp} , and ρ_{ms} as the quantum channel. I employ the Bell-state measurement scheme for the multiphoton qubits proposed in Ref. [34]. Its schematic diagram is presented in Fig. 4. In the multiphoton qubit encoding, the Bell

states are defined as

$$\begin{aligned} |B_{1,2}^N\rangle &= \frac{1}{\sqrt{2}} \left(|H\rangle^{\otimes N} |H\rangle^{\otimes N} \pm |V\rangle^{\otimes N} |V\rangle^{\otimes N} \right), \\ |B_{3,4}^N\rangle &= \frac{1}{\sqrt{2}} \left(|H\rangle^{\otimes N} |V\rangle^{\otimes N} \pm |V\rangle^{\otimes N} |H\rangle^{\otimes N} \right), \end{aligned} \quad (2.18)$$

where \pm is chosen in the same order of the two number labels of $|B_i^N\rangle$ in each line. Let us denote the i th photons of each party as $|\cdot\rangle_i$ and $|\cdot\rangle_{i'}$. I pairwise measure $|\cdot\rangle_i |\cdot\rangle_{i'}$ by the standard 2-photon Bell-state measurement scheme as

$$\begin{aligned} |H\rangle_i |H\rangle_{i'} &= \frac{1}{\sqrt{2}} (|B_1\rangle_{ii'} + |B_2\rangle_{ii'}), & |V\rangle_i |V\rangle_{i'} &= \frac{1}{\sqrt{2}} (|B_1\rangle_{ii'} - |B_2\rangle_{ii'}), \\ |H\rangle_i |V\rangle_{i'} &= \frac{1}{\sqrt{2}} (|B_3\rangle_{ii'} + |B_4\rangle_{ii'}), & |V\rangle_i |H\rangle_{i'} &= \frac{1}{\sqrt{2}} (|B_3\rangle_{ii'} - |B_4\rangle_{ii'}). \end{aligned}$$

Therefore, the Bell-state measurement of the multiphoton qubit is represented by the N Bell-state measurements of the PSP qubit as

$$|B_{1,2}^N\rangle = \frac{1}{\sqrt{2^{N+1}}} \left(\prod_i (|B_1\rangle_{ii'} + |B_2\rangle_{ii'}) \pm \prod_i (|B_1\rangle_{ii'} - |B_2\rangle_{ii'}) \right), \quad (2.19)$$

$$|B_{1,2}^N\rangle = \frac{1}{\sqrt{2^{N+1}}} \left(\prod_i (|B_3\rangle_{ii'} + |B_4\rangle_{ii'}) \pm \prod_i (|B_3\rangle_{ii'} - |B_4\rangle_{ii'}) \right). \quad (2.20)$$

I choose that $|B_1\rangle$ and $|B_3\rangle$ is the identifiable outcomes so that the measurement results can be B_1 , B_3 , or ambiguous outcome of B_2 or B_4 . From Eq. (2.20), $|B_1^N\rangle$ and $|B_3^N\rangle$ consist of an even number of $|B_2\rangle$ and $|B_4\rangle$ while $|B_2^N\rangle$ and $|B_4^N\rangle$ do of an odd number. For example, after N measurements, if B_1 occurs at least one time and the ambiguous results are odd times, I conclude

the input is B_2 . Therefore, the failure event is when all measurement results are ambiguous, which occurs with a average probability $1 - 1/2^N$ assuming the four Bell states come with a uniform probability $1/4$. This scheme only use linear optics and on-off photodetectors.

When one or more photons are lost from the multiphoton qubit in hybrid entangled states, there is a chance that $|B_i^K\rangle$ with $K < N$ is detected. However, although I accept these events as a success, the fidelity is not improved. I pointed out earlier that ρ^{loss} does not contain entanglement due to the dephasing induced by photon loss. The teleportation fidelity between the input and output qubits cannot then exceed the classical limit, which I will discuss further at the end of this section. I thus take only the detection of N -photon Bell states as the successful events.

Similarly to the standard teleportation scheme, a sender jointly measures the input state of a multiphoton qubit $|\psi_{\text{in}}\rangle = a|H\rangle^{\otimes N} + b|V\rangle^{\otimes N}$ and the multiphoton-qubit part of the hybrid entangled states on the multiphoton Bell-state basis in Eq. (2.18). After the Bell-state measurement with outcome i , the input state $|\psi_{\text{in}}\rangle$ and the hybrid entangled state under photon loss, $\rho_{\text{hyb}}(t_M, t_C)$, are projected to

$$\rho_{\text{out},i}(t_M, t_C) = \frac{\langle B_i^N | (|\psi_{\text{in}}\rangle\langle\psi_{\text{in}}| \otimes \rho_{\text{hyb}}(t_M, t_C)) | B_i^N \rangle}{\text{tr}[|B_i^N\rangle\langle B_i^N| (\psi_{\text{in}} \otimes \rho_{\text{hyb}}(t_M, t_C))]} \quad (2.21)$$

With the heralded measurement outcome i , the receiver may recover the state $\rho_{\text{out}} = \rho_{\text{out},1}$ by a proper local unitary based on the outcome i .

Before proceeding further, I point out that the output state does not depend on loss η_M on the multiphoton-qubit part. The hybrid entangled state

can be represented as $\rho_{\text{hyb}}(t_M, t_C) = t_M^{2N} \sigma_{\text{hyb}}(t_C) + \rho^{\text{loss}}$, where $\sigma_{\text{hyb}}(t_C)$ corresponds to the state when no photon is lost from the multiphoton qubit. The factor t_M^{2N} indicates that this event happens with a probability of $t_M^{2N} = (1 - \eta_M)^N$. Since the loss term ρ^{loss} is orthogonal to the qubit basis $\{|H\rangle^{\otimes N}, |V\rangle^{\otimes N}\}$, only $\sigma_{\text{hyb}}(t_C)$ remains after the projection on $|B_N^i\rangle$. The factor t_M^{2N} in both the numerator and the denominator of Eq. (2.21) then cancels out. Thus, $\rho_{\text{out}}(t_M, t_C)$ is independent of t_M so that it can be represented as $\rho_{\text{out}}(t_C)$.

I set the target state of the teleportation to be $|\psi_t\rangle = a|C_0\rangle + b|C_1\rangle$. The quantum fidelity between the output state ρ_{out} and the target state $|\psi_t\rangle$ is defined as

$$F(t_C) = \langle \psi_t | \rho_{\text{out}}(t_C) | \psi_t \rangle.$$

Now, I examine the candidates of the carrier qubit. First, I consider quantum teleportation from a multiphoton qubit to a coherent-state qubit. When $|B_1^N\rangle$ is detected, I can express the output qubits after Bell-state measurement by

$$\begin{aligned} \rho_{\text{out},1}^{\text{m} \rightarrow \text{c}} = & M_+ \left[|a|^2 |t_C \alpha\rangle \langle t_C \alpha| + |b|^2 | -t_C \alpha\rangle \langle -t_C \alpha| \right. \\ & \left. + e^{-2\alpha^2 r_c^2} (ab^* |t_C \alpha\rangle \langle -t_C \alpha| + \text{H.c.}) \right], \end{aligned}$$

where $M_+ = [1 + e^{-2\alpha^2} (ab^* + a^*b)]^{-1}$. When $|B_3^N\rangle$ is detected, the output qubit undergoes a bit flip as $\rho_{\text{out},3}^{\text{m} \rightarrow \text{c}} = X_c \rho_{\text{out},1}^{\text{m} \rightarrow \text{c}} X_c^\dagger$ with $X_c : |\pm t_C \alpha\rangle \rightarrow |\mp t_C \alpha\rangle$. This effect can be corrected by applying a π -phase shifter. However, when

$|B_2^N\rangle$ is detected, the output qubit becomes

$$\begin{aligned} \rho_{\text{out},2}^{\text{m} \rightarrow \text{c}} = & M_- \left[|a|^2 |t_C \alpha\rangle \langle t_C \alpha| + |b|^2 |-t_C \alpha\rangle \langle -t_C \alpha| \right. \\ & \left. - e^{-2\alpha^2 r_C^2} (ab^* |t_C \alpha\rangle \langle -t_C \alpha| + \text{H.c.}) \right], \end{aligned}$$

which cannot be corrected to $\rho_{\text{out},1}^{\text{m} \rightarrow \text{c}}$ by applying a unitary operation because of the nonorthogonality of the coherent-state qubit basis. In other words, the required operation $Z_c : |\pm t_C \alpha\rangle \rightarrow \pm |\pm t_C \alpha\rangle$ cannot be performed in a fully deterministic way. There are, however, approximate methods to perform the required Z_c operation using the displacement operation [26, 37] or the gate teleportation protocol [38]. I also note that the transformation of $\rho_{\text{out},4}^{\text{m} \rightarrow \text{c}} \rightarrow \rho_{\text{out},2}^{\text{m} \rightarrow \text{c}}$ can be carried out by the X_c gate. Therefore, the output qubit is one of the non-exchangable states, $\rho_{\text{out},1}^{\text{m} \rightarrow \text{c}}$ or $\rho_{\text{out},2}^{\text{m} \rightarrow \text{c}}$. I denote these two states as $\rho_{\text{out},\pm}^{\text{m} \rightarrow \text{c}}$. Nevertheless, the measurement outcome i heralds the transformation of the output states. Thus, the output qubit has the quantum information of the initial qubit.

Given the transmittance t_C , I take the dynamical qubit basis $\{|t_C \alpha\rangle, |-t_C \alpha\rangle\}$ as the output qubit basis. As an analogy of the input state, I set the two target states as

$$|\Psi_{t,\pm}^{\text{m} \rightarrow \text{c}}\rangle = N_{\pm} (a |t_C \alpha\rangle \pm b |-t_C \alpha\rangle),$$

where $N_{\pm} = \{1 \pm (ab^* + a^*b) \exp(-2t^2 \alpha^2)\}^{-1/2}$ are the normalization con-

stants. Then, I obtain the fidelity between $\rho_{\text{out},\pm}^{m \rightarrow c}$ and $|\psi_{t,\pm}^{m \rightarrow c}\rangle$ respectively:

$$\begin{aligned} F_{\pm}^{m \rightarrow c}(t_C; a, b) &= \langle \psi_{t,\pm}^{m \rightarrow c} | \rho_{\text{out},\pm}^{m \rightarrow c} | \psi_{t,\pm}^{m \rightarrow c} \rangle \\ &= M_{\pm} N_{\pm}^2 [|a|^2 |a \pm bS|^2 + |b|^2 |aS \pm b|^2 \pm 2e^{-2\alpha^2 r_C^2} \text{Re}[ab^*(a^* \pm b^*S)(aS \pm b)]], \end{aligned}$$

where $S = \langle t_C \alpha | -t_C \alpha \rangle = e^{-2t_C^2 \alpha^2}$ is the overlap between the output coherent-state qubit basis states. The average fidelity is now computed over all input states. I use a parametrization $a = \cos(\theta/2) \exp(i\phi/2)$ and $b = \sin(\theta/2) \exp(-i\phi/2)$ with uniformly random sampling on the Bloch sphere. Note that $F_{+}^{m \rightarrow c}(t_C; a, b) = F_{-}^{m \rightarrow c}(t_C; a, -b)$, so the average fidelities of both cases are equal. Finally, I get the following integration:

$$\begin{aligned} F_{\text{ave}}^{m \rightarrow c}(t_C) &= \langle F_{\pm}^{m \rightarrow c}(t_C; a, b) \rangle_{\theta, \phi} \\ &= \frac{1}{4\pi} \int_0^{\pi} d\theta \sin \theta \int_0^{2\pi} d\phi F_{\pm}^{m \rightarrow c}(t_C; \theta, \phi). \end{aligned} \quad (2.22)$$

The analytic expression of this integration is given in Ref. [39] but is too lengthy to present here. I show the average fidelity varying amplitude α of the coherent-state qubit in Fig. 5 (a). The plot shows that as the mean photon number α^2 is smaller, the average fidelity approaches the unity. However, a small value of α makes the overlap between $|\pm\alpha\rangle$ large so that its ability for quantum information processing (for example, the probability to perform Z_c gate) becomes low.

In the case of the quantum teleportation from multiphoton qubit to PSP qubit, I use the hybrid entangled state in Eq. (2.15). Since all single-qubit

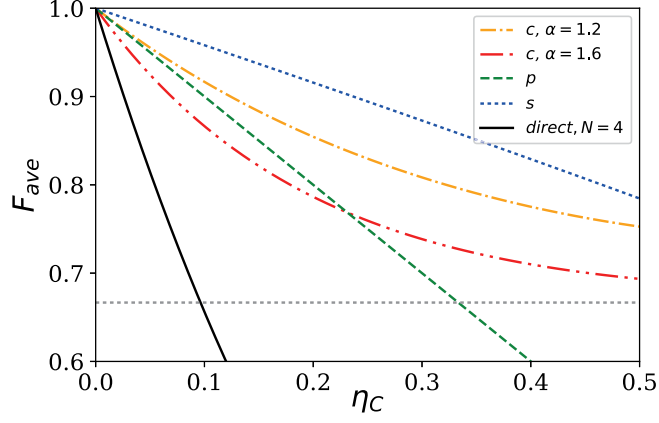


Figure 5: Average fidelities of direct transmission with $N = 4$ (black solid) and hybrid architectures with different carrier qubits: coherent state qubits (denoted by c) for $\alpha = 1.2$ (yellow dot-dashed) and $\alpha = 1.6$ (red dot-dot-dashed), a PSP qubit (p , green dashed), and a VSP qubit (s , blue dotted) against the photon-lose rate for the carrier-qubit part $\eta_c = 1 - t_c^2$. The gray horizontal dotted line is the classical limit $F_{cl} = 2/3$.

operations can be implemented in linear optics [8, 23], I set the unique target state: $|\psi_t^{m \rightarrow p}\rangle = a|H\rangle + b|V\rangle$. When a Bell state $|B_1^N\rangle$ is detected, the output state is

$$\begin{aligned} \rho_{\text{out},1}^{m \rightarrow p} &= t_C^2 (|a|^2 |H\rangle\langle H| + |b|^2 |V\rangle\langle V| + ab^* |H\rangle\langle V| + a^*b |V\rangle\langle H|) + r_C^2 |0\rangle\langle 0| \\ &= t_C^2 |\psi_t^{m \rightarrow p}\rangle\langle \psi_t^{m \rightarrow p}| + r_C^2 |0\rangle\langle 0|. \end{aligned}$$

When the other Bell states are detected, after receiving the measurement outcome, the receiver can recover the target state by a proper single-qubit unitary operation. The fidelity is then readily obtained as

$$F^{m \rightarrow p}(t_C) = t_C^2.$$

The last case is teleportation from a multiphoton qubit to a VSP qubit with the entangled state in Eq. (2.16). In this case of the VSP qubit, the situation is similar to the case of the coherent-state qubit. While the Z operation is deterministic in linear optics, the X operation, $X : |0\rangle \leftrightarrow |1\rangle$, is probabilistic [25]. Therefore, I distinguish the output qubit of $|B_1^N\rangle$ detection, denoting $\rho_{\text{out},+}^{m \rightarrow s}$, from $|B_2^N\rangle$, denoting $\rho_{\text{out},-}^{m \rightarrow s}$. The output qubit when $|B_1^N\rangle$ is detected is obtained similarly as

$$\rho_{\text{out},+}^{m \rightarrow s} = (|a|^2 + |b|^2 r_C^2) |0\rangle\langle 0| + |b|^2 t_C^2 |1\rangle\langle 1| + (ab^* t_C |0\rangle\langle 1| + \text{H.c.}).$$

I then obtain the input-dependent fidelity as

$$F^{m \rightarrow s}(t_C) = |a|^4 + |a|^2 |b|^2 (1 + t_C) + |b|^4 t_C^2.$$

In this case, the average fidelity has a simple analytic expression:

$$F_{\text{ave}}^{m \rightarrow s}(t_C) = \frac{1}{3} t_C^2 + \frac{1}{6} t_C + \frac{1}{2}.$$

I need to consider the classical fidelity F_{cl} that is defined as the maximum average fidelity obtained by teleportation protocol without entanglement. It is well known that $F_{\text{cl}} = 2/3$ for a qubit with an orthonormal basis [40]. If I use the coherent-state qubit of $|\pm\alpha\rangle$ as the carrier qubit, however,

$F_{\text{cl}}^{\text{m} \rightarrow \text{c}}$ is

$$F_{\text{cl}}^{\text{m} \rightarrow \text{c}}(t_C) = \frac{S + 3S^2 - (S^4 - 1)}{4S^3} \sinh^{-1} \left[\frac{S}{\sqrt{1 - S^2}} \right],$$

where $S = \langle -t_C \alpha | t_C \alpha \rangle = e^{-2t_C^2 \alpha^2}$ [39]. In this case, the classical limit becomes larger $2/3$ due to the nonorthogonality S . Of course, $F_{\text{cl}}^{\text{m} \rightarrow \text{c}}$ converges to $2/3$ as $S \rightarrow 0$. In Fig. 5, the average fidelity $F_{\text{cl}}^{\text{m} \rightarrow \text{c}}$ is approximately $2/3$ for the area of $\alpha \geq 1.2$ and $\eta \leq 0.5$.

In Fig. 5, I present the average fidelities between the output qubit and the target state against the photon-loss rate η_C for the different types of the carrier qubit. For the coherent-state qubit, I choose amplitudes of $\alpha = 1.2$ and 1.6 , which are approximately the minimum and optimal amplitudes, respectively, for the fault-tolerant quantum computing using the 7-qubit Steane code [41]. Obvious, better fidelities over the direct transmission can be obtained using the teleportation protocol. Among the carrier qubits, the VSP qubit is better than the PSP qubit. The reason for this can be understood as follows. When photon loss occurs, the PSP qubit gets out of the original qubit space because of the vacuum portion. However, the VSP qubit remains in the original qubit space even under the photon loss.

The comparison between the coherent-state qubit and the other types of qubits depends on amplitude α . With small values of α , the coherent-state qubit shows higher average fidelity than the others. I numerically obtain that, when $\alpha < 1.23$ ($\alpha < 0.78$), the average fidelity of the corresponding coherent-state qubit is higher than that of the PSP qubit (the VSP qubit) for any rates of photon loss. However, one should note that the overlap be-

Table 1: Maximum photon-loss rates for the carrier qubit, η_C , required to reach the fidelity of 99.9%, 99%, and 90% with the coherent-state (CS) qubit, the PSP qubit, and the VSP qubit. The direct transmission (DT) of the multiphoton qubit with the photon number $N = 4$ is given for comparison under the same photon-loss rate.

F	DT	CS		PSP	VSP	
		1.2	1.6			
99.9%	0.025	0.10	0.059	0.10	0.24	
99%	0.25	1.1	0.59	1.0	2.4	$(\times 10^{-2})$
90%	2.6	12	7.0	10	24	

tween two coherent states $|\pm\alpha\rangle$ is $\langle\alpha|-\alpha\rangle = \exp(-2\alpha^2) \approx 0.0485$ (0.296) for $\alpha = 1.23$ (0.78), which could be a negative factor depending on the task to perform.

In Table 1, I summarize the maximum photon-loss rates for the carrier qubit, η_C , which can be tolerated while preserving the fidelity to be 99.9%, 99%, and 90% within our hybrid architectures. In this high fidelity regime, the VSP qubit tolerates approximately 10 times larger photon loss than the direct transmission.

2.4.4 Success probabilities

Only when the input qubits are in the logical qubit basis and the identification between $|B_1^N\rangle$ and $|B_3^N\rangle$ is successful, the Bell-state measurement successes. Let us denote q_i as the probability of the successful identification of $|B_i^N\rangle$ when $|B_i^N\rangle$ is given. This q_i varies according to the Bell-state measurement scheme, and I follows the Bell-state measurement scheme of multiphoton qubit that $q_i = 1 - 1/2^{N-1}$ for $i = \text{odd}$ and $q_i = 1$ for $i = \text{even}$

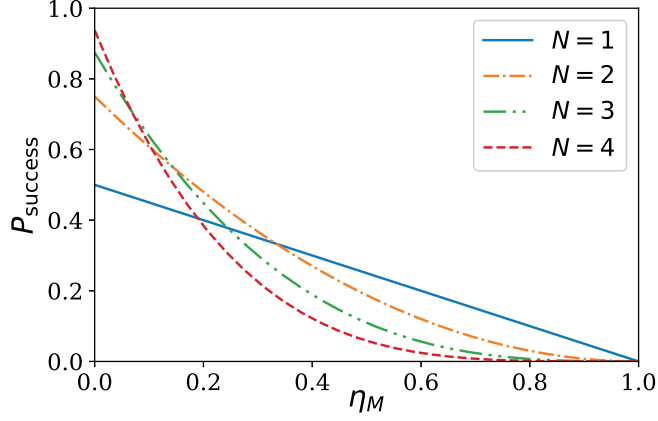


Figure 6: Success probability P_{success} of the multiphoton Bell-state measurement against the photon-loss rate for the multiphoton qubit $\eta_M = 1 - t_M^2$ for photon numbers of $N=1, 2, 3$, and 4.

[34]. The success probability of the teleportation with the hybrid entangled state ρ_{hyb} is then given as

$$P = \sum_i q_i \text{tr} \left[|B_i^N\rangle_{SS'} \langle B_i^N| (|\psi_{\text{in}}\rangle_S \langle \psi_{\text{in}}| \otimes (\rho_{\text{hyb}})_{S'R}) \right], \quad (2.23)$$

where S and S' represents the sender's modes and R does the receiver's mode. Note that the success probability P does not depend on t_C since

$$\begin{aligned} & \text{tr} \left[|B_i^N\rangle_{SS'} \langle B_i^N| (|\psi_{\text{in}}\rangle_S \langle \psi_{\text{in}}| \otimes (\rho_{\text{hyb}})_{S'R}) \right] \\ &= \text{tr}_{SS'} \left[|B_i^N\rangle_{SS'} \langle B_i^N| (|\psi_{\text{in}}\rangle_S \langle \psi_{\text{in}}| \otimes (\text{tr}_R \rho_{\text{hyb}})_{S'}) \right] \end{aligned}$$

and $\text{tr}_R \rho_{\text{hyb}}(t_M, t_C) = \text{tr}_R (\Phi_{t_M} \otimes I) (|\psi_{\text{hyb}}\rangle \langle \psi_{\text{hyb}}|)$ from the trace-preserving property of Φ_t where R represents the receiver's mode and Φ_{t_M} is the quantum channel of photon loss with transmittance t_M .

Now, I examine the success probability for each carrier qubit. For the case of teleportation to a coherent-state qubit with ρ_{mc} in Eq. (2.14), the success probability of the teleportation, $P^{m \rightarrow c}$, is obtained using Eq. (2.23) as

$$P^{m \rightarrow c}(t_M, N; a, b) = t_M^{2N} \left[\left(1 - \frac{1}{2^N} \right) - \frac{e^{-2\alpha^2}}{2^N} (ab^* + a^*b) \right].$$

The last term is from the nonorthogonality of the coherent state qubit. I also obtain the averaged success probability $P_{\text{ave}}^{m \rightarrow c}$ by averaging $P^{m \rightarrow c}(t_M, N; a, b)$ on all possible input state with the same parametrization of Eq. (2.22) as

$$P_{\text{ave}}^{m \rightarrow c}(t_M, N) = t_M^{2N} \left(1 - \frac{1}{2^N} \right).$$

For the discrete variable qubits, I have $\text{tr}_R(\Phi_{t_M} \otimes I) |\psi_{\text{hyb}}\rangle \langle \psi_{\text{hyb}}| = \Phi_{t_M}(I/2)$. Therefore, without dependence on the carrier qubit, I obtain

$$P(t_M, N) = t_M^{2N} \left(1 - \frac{1}{2^N} \right). \quad (2.24)$$

In Fig. 6, I plot the success probability $P(t_M, N)$ as a function of the photon loss rate for the multiphoton qubit, η_M , by changing the photon number N of the multiphoton qubit. The success probability in Eq. (2.24) shows an interesting feature: while the success probability of Bell-state measurement increases with N for $t_M = 1$, if t_M is less than 1, larger N rather makes the success probability lower. This supports the general belief that a “macroscopic object” is fragile under loss if I regard the larger N means the qubit

is more “macroscopic” [42]. It is straightforward to obtain the optimal number of photons per a multiphoton qubit, $N_{\text{opt}} = \lfloor \log_2(1 + 1/\eta_M) \rfloor$, that maximizes the success probability $P(t_M, N)$.

2.5 Generation of hybrid entangled states

In this section, I discuss how to generate the hybrid entangled states $|\psi_{\text{sc}}\rangle$ in Eq. (2.3) and $|\psi_{\text{mc}}\rangle$, $|\psi_{\text{mp}}\rangle$ and $|\psi_{\text{ms}}\rangle$ in Eq. (2.13).

First, let me discuss the hybrid entangled state between a VSP qubit and coherent-state qubit $|\psi_{\text{sc}}\rangle$. This hybrid entangled state is experimentally generated in Ref. [32, 43]. Here, I review the most relative scheme [32]. The conceptual schematic is presented in Fig. 7 (a). The essential procedure of this scheme is to implement a superposition of creation operators

$$ra_1^\dagger + ta_2^\dagger, \quad (2.25)$$

where $|t|^2 + |r|^2 = 1$. A single-mode creation operator a^\dagger is implemented using a parametric downconverter, which is heralded when a idler photon is detected. To make two creation operators superposed, the information of the location that the creation occurs is erased using a beamsplitter on two idler photons. The operator in Eq. (2.25) is, then, applied on the input state $|0\rangle_1 |\alpha_i\rangle_2$. The resulting state is

$$|\psi\rangle_{12} = \frac{1}{\sqrt{2}} \left(|1\rangle_1 |\alpha_i\rangle_2 + |0\rangle_1 \frac{a^\dagger}{\sqrt{|\alpha_i|^2 + 1}} |\alpha_i\rangle_2 \right), \quad (2.26)$$

when they choose $t = \sqrt{\frac{1+|\alpha_i|^2}{2+|\alpha|^2}}$. It is known that the photon-added state is a good approximation of a coherent state with a large amplitude as $\frac{a^\dagger}{\sqrt{|\alpha|^2+1}}|\alpha\rangle \approx |g\alpha\rangle$ where $g = \frac{1}{2} + \sqrt{\frac{1}{4} + \frac{1}{|\alpha|^2}}$. The fidelity is given by $F = g^2 \frac{|\alpha|^2}{|\alpha|^2+1} e^{-|\alpha|^2(g-1)^2}$. Therefore, Eq. (2.26) is a superposition with α and $g\alpha$. Finally, a displacement operator $D(-\frac{g+1}{2}\alpha_i)$ is applied on the mode 2 so that they obtain the desired hybrid state as

$$|\Psi_{sc}\rangle = D(-\frac{\alpha+g\alpha}{2})|\Psi\rangle_{12} \approx \frac{1}{\sqrt{2}}(|1\rangle_1 |-\alpha_f\rangle_2 + |0\rangle_1 |\alpha_f\rangle_2), \quad (2.27)$$

where $\alpha_f = \frac{g-1}{2}\alpha_i$. The final amplitude α_f becomes larger with a smaller α_i . However, the small α_i makes the fidelity of $a^\dagger|\alpha_i\rangle \approx |g\alpha_i\rangle$ low. They showed that starting with $\alpha_i = 2$, $F \approx 0.991$ and $\alpha_f \approx 0.21$, but with $\alpha_i = 1$, $F \approx 0.946$ and $\alpha_f = 0.31$.

Second, for the generation of $|\Psi_{mc}\rangle$, $|\Psi_{mp}\rangle$ and $|\Psi_{ms}\rangle$, I may start with a GHZ state of PSP qubits:

$$|\text{GHZ}(N)\rangle = (|H\rangle^{\otimes N} + |V\rangle^{\otimes N})/\sqrt{2}$$

It is then clear that $|\Psi_{mp}\rangle = (|H\rangle^{\otimes N}|H\rangle + |V\rangle^{\otimes N}|V\rangle)/\sqrt{2}$ is simply a GHZ state with $N+1$ modes $|\text{GHZ}(N+1)\rangle$. In addition to a GHZ state of $N+1$ photons $|\text{GHZ}(N+1)\rangle$, I need to find out methods to convert one of the polarization qubits in the GHZ state to the desired carrier qubit by a conversion gate

$$V = |C_0\rangle\langle H| + |C_1\rangle\langle V|.$$

In this way, desired hybrid entangled states may be obtained.

There are a number of proposals for the generation of the GHZ state. A linear optical setup, called the (Type-I) fusion gate, is designed to fuse $|\text{GHZ}(N)\rangle$ and $|\text{GHZ}(2)\rangle$ to generate $|\text{GHZ}(N+1)\rangle$ with a probability of 50% [44]. In a similar method (Supplementary Material of Ref. [45]), 6 single photons are fused by the fusion gate followed by a Bell-state projection to generate $|\text{GHZ}(3)\rangle$. The Bell-state measurements on copies of $|\text{GHZ}(3)\rangle$ also provide a probabilistic method to generate a GHZ state with an arbitrary high photon number [45, 46]. Using the Bell-state measurements, this method is made robust to photon loss [45]. Alternatively, a method based on a nonlinear interaction, called coherent photon conversion, was proposed to implement a deterministic photon-doubling gate $|HH\rangle\langle H| + |VV\rangle\langle V|$ [47]. So far, the multiphoton GHZ-type entanglement has been experimentally observed with postselection in most experiments (for example, [48, 49, 50, 51, 52]), which cannot be used as a teleportation channel. Nevertheless, a direct generation of a three-photon GHZ state was experimentally performed [53].

Several methods converting one single-photon polarization qubit to the vacuum-and-single-photon qubit have been proposed [54, 55, 56]. Figure 7 (b) depicts the technique proposed in Ref. [56], where the conversion gate $V_{s \rightarrow p} = |0\rangle\langle H| + |1\rangle\langle V|$ was experimentally demonstrated by bell-state measurement and post-selection. They use a two-mode squeezed vacuum state $|\text{TMSV}_{VH}\rangle_{1,2} = \sqrt{1-\gamma^2} \sum_{n=0}^{\infty} \gamma^n |n_V, n_H\rangle_{1,2}$ and a polarized coherent state $|\alpha_V\rangle_3 = e^{-|\alpha|^2/2} \sum_n \frac{\alpha^n}{\sqrt{n!}} |n_V\rangle$ as resource states where γ is a squeezing parameter and α is an amplitude of the coherent state. Here, n_H and n_V denote the photon numbers in the horizontal and vertical modes. They choose the

amplitude $\alpha = \gamma$ so that the lights in the mode 2 and 3 are combined to a single spatial mode 2' by a polarizing beam splitter(PBS), which reflects only the vertical polarized photon, as

$$\begin{aligned} |\text{TMSV}_{VH}\rangle_{1,2} |\alpha_V\rangle_3 &\propto |0,0,0\rangle_{1,2,3} + \gamma |1_V, 1_H, 0\rangle_{1,2,3} + \gamma |0,0,1_V\rangle_{1,2,3} + O(\gamma^2) \\ &\rightarrow |\Omega\rangle \propto |0,0\rangle_{1,2'} + \gamma |0,1_V\rangle_{1,2'} + \gamma |1_V, 1_H\rangle_{1,2'} + O(\gamma^2). \end{aligned}$$

Then, the following setup jointly projects the mode 2' and input state on $|\psi_{\pm}\rangle = \frac{1}{\sqrt{2}}(|1_H, 1_V\rangle \pm |1_V, 1_H\rangle)$. When $|\psi_+\rangle$ is measured, the second and third terms in $|\Omega\rangle$ serve, and the output state is transformed as $V_{p \rightarrow s} |\psi_{\text{in}}\rangle$ where $V_{p \rightarrow s} = |0_V\rangle\langle 1_H| + |1_V\rangle\langle 1_V|$. When $|\psi_-\rangle$, the output qubit is bit-flipped. In the ideal situation where no photon is lost, the success probability is given by $P[V_{p \rightarrow s}](\gamma) = \gamma^4(1 - \gamma^2)e^{-\gamma^2}/4$ determined by the squeezing parameter of the two-mode squeezed state. The maximum of the success probability is $P[V_{p \rightarrow s}](\gamma^*) \approx 1.98\%$ where $\gamma^* = 2 - \sqrt{2} \approx 0.586$.

In Ref. [57], the authors suggest a method for conversion operation $V_{p \rightarrow c} = |\alpha\rangle\langle H| + |-\alpha\rangle\langle V|$ using linear optics with single-photon detectors that can distinguish a single photon from two. The resource state is an optical (Schrödinger) cat state, $|\text{SCS}(\alpha/t)\rangle = A(\alpha/t)(|\alpha/t\rangle + |-\alpha/t\rangle)$, where $A(\alpha) = (2 + 2e^{-2\alpha^2})^{-1/2}$ is the normalization factor. In Figure 7 (c), the schematic diagram is described. The optical cat state is split into the two-mode state $|\alpha\rangle_2 |\beta\rangle_3 + |-\alpha\rangle_2 |-\beta\rangle_3 = |\alpha\rangle_2 D_3(\beta) |0\rangle_3 + |-\alpha\rangle_2 D_3(-\beta) |0\rangle_3$ via a beam splitter(BS) with transmittance t where $\beta = r\alpha/t$ and $D(\beta) = \exp(\beta a^\dagger - \beta^* a)$. At the same time, the input state is displaced by $D_4(\beta)$. Then, through a beam splitter, the displacement in the mode 3 and 4 are

interfered as $D_3(\beta)D_4(\beta) \rightarrow D_{3'}(\sqrt{2}\beta)$ and $D_3(-\beta)D_4(\beta) \rightarrow D_{4'}(-\sqrt{2}\beta)$. Meanwhile, a single-photon polarization qubit $|\psi_{\text{in}}\rangle = c_H|H\rangle + c_V|V\rangle$ becomes equally superposed in the mode 3' and 4' as $U_{\text{BS}}|\psi_{\text{in}}\rangle = (|\psi_{\text{in}}\rangle_{3'} + |\psi_{\text{in}}\rangle_{4'})/\sqrt{2}$. Before the measurement, the total state is then proportional to

$$|\alpha\rangle_2 (|\phi_{\text{in}}\rangle_{3'}|0\rangle_{4'} + |\sqrt{2}\beta\rangle_{3'}|\psi_{\text{in}}\rangle_{4'}) + |-\alpha\rangle_2 (|\psi_{\text{in}}\rangle_{3'}|-\sqrt{2}\beta\rangle_{4'} + |0\rangle_{3'}|\phi_{\text{in}}\rangle_{4'}),$$

where $|\phi_{\text{in}}\rangle = D(\beta)|\psi_{\text{in}}\rangle$. The heralded transform $V_{\text{p} \rightarrow \text{c}}$ occurs conditioned on the detection $\Pi = |1_V\rangle\langle 1_V|_{3'} \otimes |1_H\rangle\langle 1_H|_{4'}$. When $\Pi' = |1_H\rangle\langle 1_H|_{3'} \otimes |1_V\rangle\langle 1_V|_{4'}$ occurs, the resulting qubit is bit-flipped. Assuming no photon loss, the success probability of the conversion $V_{\text{p} \rightarrow \text{c}}$ is $P[V_{\text{p} \rightarrow \text{c}}](t, \alpha) = \langle \Pi \rangle = A(\alpha/t)^2(\frac{1}{t^2} - 1)\alpha^2 e^{-2(1/t^2 - 1)\alpha^2}$. If the bit-flip is allowed, the success probability becomes double. This scheme allows the conversion $V_{\text{p} \rightarrow \text{c}} = |\alpha\rangle\langle H| + |-\alpha\rangle\langle V|$ using an optical cat state with an amplitude slightly larger than α . Within our knowledge, the recent record of the amplitude of the optical cat state is $\alpha = 1.85$ [58]. Therefore, I can obtain a hybrid entangled state between a multiphoton qubit and a coherent-state qubit with $\alpha < 1.85$, which is enough to show the robustness of the teleportation scheme for qubit transmission.

2.6 Remarks

It is important to identify an efficient qubit encoding for a given quantum information task. For example, the many-photon encoding enables one to perform a nearly deterministic Bell-state measurement, which is a remarkable advantage for quantum communication and computation. However, a many-photon qubit is vulnerable to photon loss and this is a formidable

obstacle particularly against long-distance quantum communication. To overcome this problem, I have suggested a teleportation scheme via hybrid entanglement between a many-photon qubit and another type of small-photon optical qubit serving as a loss-tolerant carrier. In our scheme, the loss-tolerant carrier qubit is sent through a lossy environment. For the coherent-state qubit case, I consider the VSP qubit, and for the multiphoton qubit, the coherent-state qubit, the PSP qubit, and the VSP qubit are considered as the loss tolerant carrier qubit.

In the case of the coherent-state qubit, I have found that the fidelity depends on both sides of the photon losses, but the loss on the coherent-state qubit side effects more severely than the opposite side due to the dephasing effect. In the extreme case where the loss occurs on only one side, the fidelity is bounded by $1/2$ from the loss on the VSP qubit side and $2/3$ by the coherent-qubit side. The success probability of the teleportation is independent of the loss on the VSP qubit side. The dependence on the coherent-state qubit side, however, is not severe: the region that the success probability is maintained is widened for large amplitude. Therefore, I conclude that the hybrid entanglement has merit mainly on the fidelity.

For the multiphoton case, I have found that the average fidelities of the teleportation with the considered hybrid entangled states are better than the direct transmission. The VSP qubit in hybrid entanglement serves as the best carrier showing about 10 times better tolerance on the photon-loss rate than the direct transmission of the multiphoton qubit for the fidelity larger than 0.9. Our numerical analysis further shows that the coherent-state qubit shows higher average fidelity than the others with small values of α . When

$\alpha < 1.23$ ($\alpha < 0.78$), the average fidelity of the corresponding coherent-state qubit is higher than that of the PSP qubit (the VSP qubit) for any rates of photon loss. These results would be useful information when choosing the proper carrier qubit depending on the quantum tasks under consideration. I have also investigated the average success probability of the teleportation. It was shown that the success probability depends only on the loss of the multiphoton-qubit part. Although the Bell-state measurement scheme of the multiphoton qubit is nearly deterministic without loss, the photon loss limits the maximum success probability.

It would be an interesting future work to construct a full quantum repeater with hybrid entanglement based on our scheme and entanglement purification protocols. For example, Sheng *et al.* [13] proposed an optical scheme for entanglement purification of hybrid entanglement that enables one to purify the bit and phase flip errors, as well as photon losses from the coherent states. Since Bell-state measurements and entanglement purification are two key elements in a quantum repeater, this work may be combined with this scheme [13] to develop a hybrid quantum repeater. Other purification schemes for carrier qubits [59, 60, 61, 62, 63, 64, 65, 11] used in our paper may be needed to construct a quantum repeater, which deserves further investigations.

The following is the publication list related to this chapter:

1. S. Choi, S.-H. Lee, and H. Jeong, “Teleportation of a multiphoton qubit using hybrid entanglement with a loss-tolerant carrier qubit,” *Phys. Rev. A* 102, 012424 (2020)

2. H. Jeong, S. Bae, S. Choi, "Quantum teleportation between a single-rail single-photon qubit and a coherent-state qubit using hybrid entanglement under decoherence effects," *Quantum Information Processing* 15, 913 (2016)

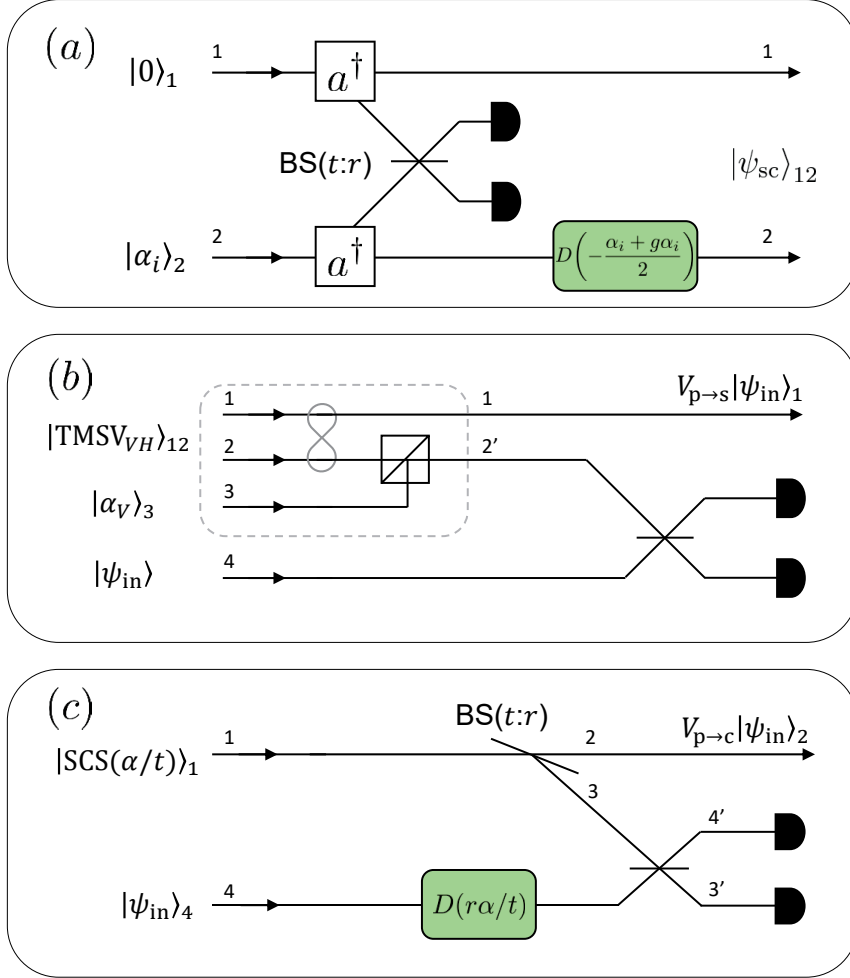


Figure 7: Conceptual schematics for (a) generating hybrid entangled state between a coherent-state qubit and VSP qubit and implementing conversion gates (b) $V_{p \rightarrow s}$ and (c) $V_{p \rightarrow c}$.

Chapter 3

Operational quantum resources beyond entanglement

3.1 Introduction

Quantum information theory reveals that quantum entanglement is a kind of resource, the requirement to achieve quantum advantages. However, it has been pointed that the quantum theory shows striking differences from the classical theory even for the single party where there is no room for the entanglement [18]. Inspired by the entanglement theory, the framework of quantum resource theory has been studied as a branch of the quantum theory, which aims to quantify a particular quantum feature in a similar way to the entanglement theory. I mainly deal with two major quantum resource theories which have great implication on the light system for the quantum information: resource theory of coherence [18] and resource theory of non-classicality [20, 21].

Quantum coherence generally refers to the generalization of the quantum superposition for the mixed state. The study of quantum resources has seen another revival of interest over the last several years due to the recent identification and characterization of a resource theory of coherence [18]. While the coherence of quantum systems has always, in some form or an-

other, been recognized as a fundamental aspect of the field [66, 67, 68], the newly developed resource theory now provides a framework that allows for a more quantitative understanding of the subject. Since this development, coherence has now been studied within the contexts of quantum correlations [69, 70, 71], macroscopic quantumness [72, 73], nonclassical light [74, 75, 76], interferometric experiments [77], quantum estimation [78], and quantum algorithms [79, 80].

On the other hand, the nonclassicality comes from an idea of the most “classical” quantum state. Given the answer, one can capture a quantum state having genuine quantum nature. For the light system, the most commonly agreed answer is the coherent state. The coherent state is initially suggested as a state minimizing the uncertainty of the position and momentum operator spontaneously [81]. It also resembles the many properties of the coherent electric field [82, 83], which make it dubbed as “coherent” state. It is known that, in a bosonic system, every quantum state can be written by a quasimixture of coherent states:

$$\rho = \int d^2\alpha P(\alpha) |\alpha\rangle\langle\alpha|, \quad (3.1)$$

where $P(\alpha)$ is referred as the Glauber-Sudarshan P function [82, 83]. Because the probabilistic mixing is generally regarded as a classical process, the quantum state whose P function is a genuine probability distribution is called classical; if not the case, the state is called nonclassical. Nonclassical states find useful applications in a wide range of tasks, such as quantum metrology[84], quantum teleportation[85], quantum cryptography[86],

quantum communication[87] and quantum information processing[88].

The resource theoretic framework, however, does not guarantee the operational meaning of the resource measure. The measures without any operational meaning have limited application on the quantum information processing: the essential requirement on the measure only provides the impossibility of a certain class of transformations. Unfortunately, many mathematically suggested measures do not have the operational meaning separated from physical effects.

In this chapter, I aim to propose the resource theoretic measure for the coherence and nonclassicality having operational meaning. I consider how to construct a coherence measure from observable quantum effects. Such effects include quantum Fisher information, related to the metrological power via Cramér-rao bound, and expectation values of observables, usually written as Hermitian operators. I also propose a computable nonclassicality measure from the negativity of the P function. This measure has an operational meaning of the robustness to the mixing with the classical state.

3.2 Measuring coherence via observable quantum effects

3.2.1 Preliminaries

I first briefly describe the formalism of quantum channels, which I take here to mean the set of all Completely Positive, Trace Preserving (CPTP) maps. There are several equivalent characterizations of quantum maps, but

for our purposes, I will be concerned with the Kraus [89] and the Choi-Jamiołkowski representations [90, 91]. In the Kraus representation, a quantum operation is represented by a map of the form $\Phi(\rho) = \sum_i K_i \rho K_i^\dagger$ which is completely specified by a set of operators $\{K_i\}$ called Kraus Operators. The Kraus operators must satisfy the completeness relation $\sum_i K_i^\dagger K_i = \mathbb{1}$ in order to qualify as a valid quantum operation. In the Choi-Jamiołkowski representation, a quantum map Φ is represented by an operator $J(\Phi) = \sum_{i,j} \Phi(|i\rangle_A \langle j|) \otimes |i\rangle_B \langle j|$ which satisfies $\text{Tr}_A[J(\Phi)] = \mathbb{1}_B$. The action of Φ on some state ρ is then recovered via the map $\text{Tr}_B[J(\Phi) \mathbb{1}_A \otimes \rho_B^T] = \Phi(\rho_A)$. A simple relationship connects both equivalent representations. For a map Φ represented by Kraus operators $\{K_i = \sum_{j,k} k_{i,j,k} |j\rangle \langle k|\}$, the corresponding Choi-Jamiołkowski representation is $J(\Phi) = \sum_i v_i v_i^\dagger$ where $v_i := \sum_{j,k} k_{i,j,k} |j\rangle |k\rangle$.

The notion of coherence that I will employ in this paper will be the one identified in [92, 18], where a set of axioms are identified to specify a reasonable measure of quantum coherence. The axioms are as follows:

For a given fixed basis $\{|i\rangle\}$, the set of incoherent states I is the set of quantum states with diagonal density matrices with respect to this basis. Incoherent completely-positive and trace-preserving maps (ICPTP) are quantum maps that map every incoherent state to another incoherent state. Consider some set of ICPTP maps O . Given this, I say that C is a measure of quantum coherence if it satisfies the following properties: (C1) (Faithfulness) $C(\rho) \geq 0$ for any quantum state ρ and equality holds if and only if $\rho \in I$. (C2a) (Weak monotonicity) C is non-increasing under any ICPTP map $\Phi \in O$, i.e., $C(\rho) \geq C(\Phi(\rho))$. (C2b) (Strong monotonicity) C is mono-

tonic on average under selective outcomes, i.e. for any ICPTP map $\Phi \in \mathcal{O}$ such that $\Phi(\rho) = \sum_n K_n \rho K_n^\dagger$, $C(\rho) \geq \sum_n p_n C(\rho_n)$, where $\rho_n = K_n \rho K_n^\dagger / p_n$ and $p_n = \text{Tr}[K_n \rho K_n^\dagger]$ for all K_n with $\sum_n K_n K_n^\dagger = \mathbb{1}$ and $K_n I K_n^\dagger \subseteq I$. (C3) (Convexity) C is convex, i.e. $\lambda C(\rho) + (1 - \lambda)C(\sigma) \geq C(\lambda\rho + (1 - \lambda)\sigma)$, for any density matrix ρ and σ with $0 \leq \lambda \leq 1$.

One may check that a particular operation is incoherent if its Kraus operators always map a diagonal density matrix to another diagonal density matrix. One important example of such an operation is the CNOT gate. I can also additionally distinguish between the maximal set of ICPTP maps, which I refer to as maximally incoherent operations (MIO) [92] from the set of ICPTP maps whose Kraus operators additionally satisfy $K_n I K_n^\dagger \subseteq I$, which I refer to as simply incoherent operations (IO) [18]. From this definition, it is clear that $\text{IO} \subset \text{MIO}$. I highlight that both MIO and IO are commonly used abbreviations and that other possible sets of ICPTP maps are also actively being considered (See [93] for examples). In this chapter, I will typically consider either MIO and IO for the set \mathcal{O} .

3.2.2 Coherence and Quantum Fisher Information

I now consider a standard metrological scenario. One first begins with the signal Hamiltonian, which is denoted θH_S . The signal Hamiltonian encodes a signal on a probe state, which is a specially prepared quantum state ρ of N particles, or more if one were to include any possible ancillary quantum particles. The Hamiltonian generates the dynamics $\rho(t) = e^{-iH_S \theta t} \rho e^{iH_S \theta t}$ and after some time $t = \tau$, a measurement is then performed on the state $\rho(\tau)$, the outcome of which is specifically designed in order to obtain the most

precise estimate of the value of θ . The optimal sensitivity is known to be given by the quantum Cramer-Rao bound [4] $\delta\theta \geq \frac{1}{\sqrt{v\mathcal{F}(\rho(\tau), H_S)}}$ where v is the number of measurements performed and $\mathcal{F}(\rho(\tau), H_S)$ is the QFI of a state with respect to H_S , given by

$$\mathcal{F}(\rho(\tau), H_S) = 2 \sum_{i,j} \frac{(\lambda_i - \lambda_j)^2}{\lambda_i + \lambda_j} |\langle i | H_S | j \rangle|^2,$$

where λ_i and $|i\rangle$ are eigenvalues and eigenstates of $\rho(\tau)$, respectively. I am primarily interested in the sensitivity of the state ρ locally at the point $t = 0$, so $\mathcal{F}(\rho, H_S)$ will be the figure of merit I will consider.

A class of Hamiltonians of particular interest is the class of *local Hamiltonians*. These Hamiltonians are a sum of N independent Hamiltonians acting on individual particles, i.e. a Hamiltonians of the form $H_S = \sum_{i=1}^N h^{(i)}$ where $h^{(i)}$ represents a nontrivial interaction acting only on the i th particle that is not proportional to the identity. I will also assume that $h^{(i)}$ does not depend on the number N . An example of a Hamiltonian of this type is a uniform magnetic field in the z direction acting on a collection of N spins, wherein this case $h^{(i)} \propto \sigma_z^{(i)}$, and $\sigma_z^{(i)}$ are the Pauli z operators acting on i th particle. As coherence is a basis dependent concept, I will adopt the basis which is naturally defined by the eigenvectors of $h^{(i)}$. This defines a set of local bases $\{|a^{(i)}\rangle\}$ for the i th particle where $a = 1, \dots, d$, and d is the dimension of the particle. Consequently, I will consider the coherence with respect to this set of local bases. Local bases were also previously studied in [69], which noted their connection with quantum correlations.

For any signal Hamiltonian of the form $H_S = \sum_{i=1}^N h^{(i)}$, and a pure

state probe $|\psi\rangle$, let us consider the maximal QFI reachable via all possible incoherent operations $\Phi \in \text{ICPTP}$ on $|\psi\rangle$, i.e. $\max_{\Phi \in \text{ICPTP}} \mathcal{F}(\Phi(|\psi\rangle\langle\psi|), H_S)$. The incoherent operation here is completely general, with no constraints otherwise. Here, I note that there is an important differentiation between N , which captures the number of particles H_S is interacting with, and the actual physical number of particles, which can be any arbitrary number so long as it is reachable via an incoherent operation.

In fact, for any coherent pure state, I can always achieve Heisenberg scaling via a suitable incoherent operation, as demonstrated by the following Lemma:

Lemma 1. *For every coherent pure state $|\psi\rangle$ and locally interacting Hamiltonian H_S , there always exists an incoherent operation Φ that achieves $\mathcal{F}(\Phi(|\psi\rangle\langle\psi|), H_S) > 0$ that scales with $O(N^2)$. The measurement that achieves this Heisenberg limited scaling can also be performed incoherently.*

Proof Let us first consider $H_S = \sum_{j=1}^N h^{(j)}$. For each $h^{(j)}$, let $|i_{\max}^{(j)}\rangle$ and $|i_{\min}^{(j)}\rangle$ be eigenvectors that corresponds to eigenvectors for the maximum and minimum eigenvalues $\lambda_{\max}(h^{(j)})$ and $\lambda_{\min}(h^{(j)})$, respectively. In this 2 dimensional subspace, let us define the Pauli operator $\sigma_x^{(j)} := |i_{\max}^{(j)}\rangle\langle i_{\min}^{(j)}| + |i_{\min}^{(j)}\rangle\langle i_{\max}^{(j)}|$.

Let $|\psi\rangle = \sum_i \sqrt{\lambda_i} |i\rangle$, where $|i\rangle$ are eigenstates of H_S which construct the incoherent basis. Without any loss in generality, I assume that the coefficients are positive real and $\lambda_1 \geq \lambda_2 \geq \dots$. I will also assume that $|i=1\rangle = |i_{\max}^{(1)}\rangle$ and $|i=2\rangle = |i_{\min}^{(1)}\rangle$ since this is just a relabelling of the basis which can be done using an incoherent unitary. The ‘extra’ particles may be con-

sidered ancillary particles that assist during the metrological process.

I now apply an incoherent CNOT type operation that performs the map $U : |\psi\rangle \rightarrow \sum_i \sqrt{\lambda_i} |i \dots i\rangle$ and then let the state evolve according to the Hamiltonian H_S . Let us now consider only the the first 2 terms of $U |\psi\rangle$, which under H_S evolves as

$$\sqrt{\lambda_1} |1 \dots 1\rangle + \sqrt{\lambda_2} |2 \dots 2\rangle \rightarrow \sqrt{\lambda_1} |1 \dots 1\rangle + \sqrt{\lambda_2} e^{i\phi\tau} |2 \dots 2\rangle$$

up to an overall phase factor. I have $\phi = \sum_{j=1}^N \phi_j$ where $\phi_j := \lambda_{\max}(h^{(j)}) - \lambda_{\min}(h^{(j)})$.

I will choose some basis on the Hilbert space space of N particles $\{|a_i\rangle\}$ for $i = 1, 2, \dots$ such that $|a_1\rangle = \frac{1}{\sqrt{2}}(|1 \dots 1\rangle + |2 \dots 2\rangle)$. Define the following POVM:

$$M_{(\vec{c}, i)} := |\pi(\vec{c}), i\rangle \prod_{j=1}^N \langle (-)^{c_j} | a_i \rangle \langle a_i|,$$

where $\vec{c} := (c_1, \dots, c_N)$, $c_j = 0, 1$, and $\pi(\vec{c}) = \prod_{j=1}^N (-1)^{c_j}$. The quantum operation \mathcal{M} is then defined as $\mathcal{M}(\rho) = \sum_{(\vec{c}, i)} M_{(\vec{c}, i)} \rho M_{(\vec{c}, i)}^\dagger$. This operation is incoherent and is effectively an incoherent implementation of 2 measurements: a projection onto the basis $\{|a_i\rangle\}$ followed by a parity measurement on the x axis. Suppose I perform the naive protocol where if the measurement outcome is $i = 1$, I keep the parity measurement outcome, and assign a value of zero otherwise. Let us call this measurement \mathcal{M}' .

I can then verify using the error propagating formula that

$$\frac{\Delta \mathcal{M}'^2}{|\partial_\tau \langle \mathcal{M}' \rangle|^2} = \frac{(\sqrt{\lambda_1} + \sqrt{\lambda_2})^2}{2} \frac{1}{\phi^2}.$$

Finally, I observe that $\phi_i \geq \phi_{\min} := \min_j \phi_j$ and $\phi \geq N\phi_{\min}$. ϕ_{\min} depends only on $\{h^{(i)}\}$, all of which do not contain any dependence on N , and neither does the coefficient $\frac{(\sqrt{\lambda_1} + \sqrt{\lambda_2})^2}{2}$, which depends only on the initial state. As such, I have

$$\frac{\Delta \mathcal{M}'^2}{|\partial_\tau \langle \mathcal{M}' \rangle|^2} \leq \frac{(\sqrt{\lambda_1} + \sqrt{\lambda_2})^2}{2} \frac{1}{N^2 \phi_{\min}} \sim O\left(\frac{1}{N^2}\right).$$

This proves that for every pure coherent state, Heisenberg limited scaling is reachable using only incoherent operations.

■

So far, I have only considered pure states and a single metrological experiment. However, I can also consider the case of general mixed states where M independent measurements are performed:

Definition 1 (Distributed coherence of QFI). *The distributed QFI for a pure state $|\Psi\rangle$ is defined to be*

$$C_F^M(|\Psi\rangle) := \max_{\Phi \in \text{ICPTP}} \sum_{i=1}^M \mathcal{F} \{ \text{Tr}_{P(i)^c} [\Phi(|\Psi\rangle \langle \Psi|)], H_S^{(i)} \}$$

where $H_S^{(i)}$ is the i th local Hamiltonian of the form $H_S^{(i)} := \sum_{j=1}^N h^{(i,j)}$ and $h^{(i,j)}$ are nontrivial. $P(i)$ refers to the i th partition of particles in the state $\Phi(|\Psi\rangle \langle \Psi|)$ which is partitioned into M collections of particles that sepa-

rately interact with the Hamiltonians $H_S^{(i)}$. The partial trace $\text{Tr}_{P(i)^c}$ is to be interpreted as tracing out every particle except the ones in $P(i)$.

The generalization to mixed states is obtained via the convex roof construction

$$C_F^M(\rho) := \min_{\{p_i, |\psi_i\rangle\}} \sum_i p_i C_F^M(|\psi_i\rangle)$$

where the minimization is over all pure state decompositions of the form $\rho = \sum_i p_i |\psi_i\rangle \langle \psi_i|$. (See [94] for another example of such constructions)

This definition corresponds to a scenario where a quantum state $\Phi(|\psi\rangle \langle \psi|)$ is prepared via an incoherent operation, partitioned into M separate subsystems, and then distributed to M different parties each performing an independent metrological experiment. Equivalently, it can also be interpreted as a single party scenario where M independent metrological experiments are performed.

It turns out that C_F^M is a valid coherence measure for every M and $H_S^{(i)}$.

Theorem 1. C_F^M is a coherence measure.

Proof I observe that if ρ is incoherent, then it is diagonal w.r.t. $\sum_i H_S^{(i)}$, and $\mathcal{F}(\rho, H_S^{(i)}) = 0$. Resorting to any incoherent operation Φ will not improve the situation as it always maps a diagonal state to another diagonal state so I must have $C_F^M(\rho) = 0$. Lemma 1 then demonstrates that if ρ is coherent, then $C_F^M(\rho) > 0$ since ρ has to have at least one pure state in its pure state decomposition that is coherent. This proves that ρ is incoherent iff $C_F^M(\rho) = 0$, so the measure is faithful.

Convexity is implied by the convex roof construction. Therefore, I only need to prove strong monotonicity.

To prove monotonicity, I only need to establish that the measure is strongly monotonic over pure states (a short proof of this fact is presented in the Appendix). I see that this is true from the following chain of inequalities:

$$\begin{aligned}
\sum_i p_i C_F^M(|\psi_i\rangle) &= \sum_i p_i C_F^M(K_i|\psi) / \sqrt{p_i} \\
&= \sum_i p_i \max_{\Phi_i \in \text{ICPTP}} \sum_{k=1}^M \mathcal{F} \{ \text{Tr}_{P(k)^c} [\Phi_i(K_i|\psi) \langle \psi | K_i^\dagger / p_i], H_S^{(k)} \} \\
&= \max_{\Phi_i \in \text{ICPTP}} \sum_i p_i \sum_{k=1}^M \mathcal{F} \{ \text{Tr}_{P(k)^c} [\Phi_i(K_i|\psi) \langle \psi | K_i^\dagger / p_i] \otimes |i\rangle \langle i|, H_S^{(k)} \otimes |i\rangle \langle i| \} \\
&= \max_{\Phi_i \in \text{ICPTP}} \sum_{k=1}^M \mathcal{F} \{ \text{Tr}_{P(k)^c} [\sum_i \Phi_i(K_i|\psi) \langle \psi | K_i^\dagger] \otimes |i\rangle \langle i|, \sum_i H_S^{(k)} \otimes |i\rangle \langle i| \} \\
&\leq \max_{\Phi \in \text{ICPTP}} \sum_{k=1}^M \mathcal{F} \{ \text{Tr}_{P(k)^c} [\Phi(|\psi\rangle \langle \psi|)], H_S^{(k)} \} \\
&= C_F^M(\rho)
\end{aligned}$$

where the inequality comes from the observation that the optimization in the third line is a special case of the optimization over Φ in the fifth line.

■

Note that it is possible to generalize the result to arbitrary signal Hamiltonians rather than the local Hamiltonians which is the focus of this article. To see this, simply set $N = 1$ so $H_S = h^{(1)}$ where $h^{(1)}$ is in principle any arbitrary nontrivial Hamiltonian. Nonetheless, the case of local Hamiltonians is interesting due to its connections with multipartite quantum correlations.

I also note that Thm. 1 applies for every H_S and M . In particular, for

the case $M = 1$, $C_F^1(\rho)$ is just the standard Fisher information, optimized overall incoherent operations performed on the state ρ . However, a closer inspection will reveal that for small M , the measure will saturate for relatively slow levels of coherence. I already see this from the fact that for $M = 1$ a maximally coherent qubit can already be converted to a GHZ state via a series of CNOT operations, which is sufficient to saturate the QFI and C_F^1 for $H_S = \sum_i \sigma_z^{(i)}$. As such, depending on the system being considered, larger values of M may lead to better coherence measures.

3.2.3 Coherence measures from quantum observables

In this subsection, I will discuss how a quantum observable M may be used to construct a coherence measure that satisfies axioms (C1)-(C3) (see Section 3.2.1). The following Theorem introduces a quantity that satisfies the strongly monotonic condition (C2b), which will prove useful when I eventually construct the coherence measure.

Theorem 2. *For any quantum observable M and quantum state ρ , the quantity*

$$\max_{\Phi \in O} \text{Tr}(M\Phi(\rho))$$

is strongly monotonic under incoherent operations, where O may be substituted with either the set of operations, maximally incoherent operation (MIO) or incoherent operation (IO).

Proof I first observe that any incoherent operation represented by some set of incoherent Kraus operators $\{K_i^{\text{IO}}\}$ is, by definition, also a maximally incoherent operation. Note that for any set of maximally incoherent opera-

tions $\{\Omega_i^{\text{MIO}} \mid \Omega_i^{\text{MIO}} \in \text{MIO}\}$, the map $\Omega(\rho) := \sum_i \Omega_i^{\text{MIO}}(K_i^{\text{IO}} \rho K_i^{\text{IO}\dagger})$ is also maximally incoherent since it is just a concatenation of the incoherent operation represented by $\{K_i^{\text{IO}}\}$, followed by performing a maximally incoherent operation Ω_i^{MIO} conditioned on the measurement outcome i . Let us assume that $\Omega_i^{\text{MIO}}(\rho_i)$ is the optimal maximally incoherent operation maximizing $\text{Tr}(M\Omega_i^{\text{MIO}}(\rho_i))$ for the state $\rho_i := K_i^{\text{IO}} \rho K_i^{\text{IO}\dagger} / \text{Tr}(K_i^{\text{IO}} \rho K_i^{\text{IO}\dagger})$, I then have the following series of inequalities:

$$\begin{aligned}
\max_{\Phi \in \text{MIO}} \text{Tr}(M\Phi(\rho)) &\geq \text{Tr}(M\Omega(\rho)) \\
&= \text{Tr}[M \sum_i \Omega_i^{\text{MIO}}(K_i^{\text{IO}} \rho K_i^{\text{IO}\dagger})] \\
&= \text{Tr}[M \sum_i p_i \Omega_i^{\text{MIO}}(\rho_i)] \\
&= \sum_i p_i \max_{\Phi_i \in \text{MIO}} \text{Tr}(M\Phi_i(\rho_i)),
\end{aligned}$$

where $\rho_i := K_i^{\text{IO}} \rho K_i^{\text{IO}\dagger} / \text{Tr}(K_i^{\text{IO}} \rho K_i^{\text{IO}\dagger})$ and $p_i := \text{Tr}(K_i^{\text{IO}} \rho K_i^{\text{IO}\dagger})$. I note that the last line is simply the expression for strong monotonicity, which proves the result for the case when O is MIO. Identical arguments apply when considering IO, which completes the proof. ■

In the above proof, I see that the optimization over MIO yields a valid coherence monotone within the regime of IO, so drawing a sharp distinction between the two sets of operations is not always necessary.

I note that satisfying strong monotonicity qualifies the quantity as a coherence monotone, but is insufficient to fully qualify it as a coherence mea-

sure. In order for that to happen, I need to demonstrate that $\max_{\Phi \in O} \text{Tr}(M\Phi(\rho)) = 0$ iff ρ is an incoherent state, and $\max_{\Phi \in O} \text{Tr}(M\Phi(\rho)) > 0$ whenever ρ is a coherent state. It is clear that this is only true for some special cases of M . However, the following theorem shows that even if M does not by itself satisfy the above conditions, it is still possible to construct a valid coherence measure using M .

Theorem 3. *Let M be some Hermitian quantum observable in a d -dimensional Hilbert space. Then there exists a basis $\{|i\rangle\}$ such that $\langle i | (M - \frac{\text{Tr}\{M\}}{d} \mathbb{1}) | i \rangle = 0$ for every $|i\rangle$.*

Furthermore, for every nontrivial quantum observable M , the quantity

$$C_M^O(\rho) := \max_{\Phi \in O} \text{Tr}[(M\Phi(\rho)) - \text{Tr}(M)/d]$$

is always a valid coherence measure w.r.t. any basis $\{|i\rangle\}$ that satisfies $\langle i | (M - \frac{\text{Tr}\{M\}}{d} \mathbb{1}) | i \rangle = 0$ for every $|i\rangle$. Since such a basis always exists, the coherence measure C_M^O also always exists. The set of quantum maps O may be substituted with either MIO or IO.

Proof I begin by observing that the matrix $M' = M - \frac{\text{Tr}\{M\}}{d} \mathbb{1}$ is trace zero. Since M' is nontrivial (not proportional to the identity operator), it implies that the sum of its positive eigenvalues and negative eigenvalues must be exactly equal. Let $\vec{\lambda} = (\lambda_1, \dots, \lambda_d)$ be the vector of eigenvalues of M' arranged in decreasing order. I recall the Schur-Horn theorem, which states that for every vector $\vec{v} = (v_1, \dots, v_d)$, there exists a Hermitian matrix with the same vector of eigenvalues $\vec{\lambda}$, but with diagonal entries $\vec{v} = (v_1, \dots, v_d)$ so long as the vectors satisfy the majorization condition $\vec{v} \prec \vec{\lambda}$. It is clear that

the zero vector $\vec{v} = (0, \dots, 0)$ always satisfies this condition. Therefore, there always exist a basis $\{|i\rangle\}$ for M' where the main diagonals are all zero, such that $\langle i|M'|i\rangle = 0$ for every $|i\rangle$, which proves the first part of the theorem. See Proposition 1 for an example of such a basis using mutually unbiased bases. Proposition 1 presents an alternative proof for the existence of such bases but it is important to note that not every basis that satisfies the condition $\langle i|M'|i\rangle = 0$ for every $|i\rangle$ is necessarily mutually unbiased.

Now, I proceed to prove that $C_M^O(\rho)$ is a coherence measure of with respect to the basis $\{|i\rangle\}$. The strong monotonicity condition is already satisfied due to Thm 2. The convexity of the measure is immediate from the linearity of the trace operation and the definition of C_M^O as a maximization over MIO or IO. Therefore, I only need to establish the faithfulness property of the measure.

In order to prove this, recall that in the basis $\{|i\rangle\}$, the diagonal elements of M' is all zero. Therefore, there always exists some projection onto a 2 dimensional space M' such that the corresponding submatrix has the form $\begin{pmatrix} 0 & r \\ r^* & 0 \end{pmatrix}$. I can assume without loss of generality that the projection is onto the subspace $\{|0\rangle, |1\rangle\}$, since at this point, the numerical labelling of the basis is arbitrary.

For some coherent quantum state ρ , there is at least one nonzero off-diagonal element. Since basis permutation is an incoherent operation, I can assume the nonzero off-diagonal element is ρ_{01} . In fact, I can assume that it is the only nonzero off-diagonal element as I can freely project onto the subspace spanned by $\{|0\rangle, |1\rangle\}$ and completely dephase the rest of the Hilbert

space via an incoherent operation, which allows us to prove the general result by only considering the 2-dimensional case. Suppose this leads to a 2-dimensional submatrix of the form $\begin{pmatrix} p_1 & a \\ a^* & p_2 \end{pmatrix}$ where a is nonzero since ρ is coherent.

Directly computing $\text{Tr} \begin{pmatrix} 0 & r \\ r^* & 0 \end{pmatrix} \begin{pmatrix} p_1 & a \\ a^* & p_2 \end{pmatrix}$, I get the expression $r^*a + a^*r = |ra|(e^{i\phi} + e^{-i\phi})$. This final quantity can always be made positive by performing the incoherent unitary that performs $|0\rangle \rightarrow |0\rangle$ and $|1\rangle \rightarrow e^{-i\phi}|1\rangle$ which is equivalent to making both a and r positive quantities. Since r is strictly positive as M' is a nontrivial matrix, this implies $ar > 0$ if ρ is a coherent state, so there always exists at least one incoherent operation Φ such that $\text{Tr}[M'\Phi(\rho)] > 0$ for every coherent state ρ .

Finally, I just observe that M' has zero diagonal elements w.r.t. the basis $\{|i\rangle\}$, so $\text{Tr}[M'\Phi(\rho)] = 0$ whenever ρ is incoherent and Φ is MIO or IO. This completes the proof. ■

Theorem 3 above establishes several facts. First, observe that since $C_M^O(\rho)$ is a coherence measure and nonnegative, $\text{Tr}[(M\rho)] - \text{Tr}(M)/d$ can only be positive when ρ is coherent (the basis is specified by the theorem). This establishes that every nontrivial observable M is, in fact, a witness of *some* form of coherence. One just needs to subtract the constant $\text{Tr}(M)/d$ from the mean value $\langle M \rangle$ to verify the presence of coherence.

Second, it establishes that if M is a coherence witness, then it can be interpreted as the lower bound of the *bona fide* coherence measure C_M^O . Recall that the measure C_M^O quantifies the operational usefulness of a quantum

state when one considers MIO or IO type quantum operations and the task is to maximize the mean value of a given observable M . Other examples of coherence measures with operational interpretations in terms of MIO or IO include the relative entropy of coherence, which quantifies the number of maximally coherent qubits you can distill using IO [95], as well as quantities considering how much entanglement and Fisher information can be extracted via MIO or IO [70, 96].

Third, Theorem 3 defines the preferred incoherent bases where the coherence is useful for optimizing $\langle M \rangle$ and shows that such bases always exist. The following proposition states that the coherence with respect to any basis that is mutually unbiased with respect to the eigenbasis of the observable M will always satisfy the necessary condition in Theorem 3.

Proposition 1. *Let $\{|\alpha_i\rangle\}$ be the complete set of eigenbases of some non-trivial quantum observable M , and let $\{|\beta_i\rangle\}$ be any complete basis that is mutually unbiased w.r.t. $\{|\alpha_i\rangle\}$. Then the basis $\{|\beta_i\rangle\}$ always satisfies $\langle \beta_i | (M - \frac{\text{Tr}\{M\}}{d} \mathbb{1}) | \beta_i \rangle = 0$ for every $|\beta_i\rangle$.*

In other words, w.r.t. any mutually unbiased basis $|\beta_i\rangle$, the diagonal elements of $M - \frac{\text{Tr}\{M\}}{d} \mathbb{1}$ is always zero.

Proof Let the dimension of the Hilbert space be d . I then have $|\langle \beta_i | \alpha_j \rangle|^2 = \frac{1}{d}$. Since $\{|\alpha_i\rangle\}$ is the complete eigenbasis of M , $M = \sum_i \lambda_i |\alpha_i\rangle \langle \alpha_i|$ and $\langle \beta_i | M | \beta_i \rangle = \sum_j \frac{\lambda_j}{d} = \frac{\text{Tr}\{M\}}{d}$. This implies that $\langle \beta_i | (M - \frac{\text{Tr}\{M\}}{d} \mathbb{1}) | \beta_i \rangle = 0$ for every $i = 1, \dots, d$, which is the required condition. Note that this can be considered an alternative proof of the first statement in Theorem 3. ■

In Theorem 3, I established the existence of a coherence measure C_M^O

but the proof is not constructive in the sense that given the observable M , it does not immediately inform us of a procedure to obtain the basis $\{|i\rangle\}$ and corresponding measure C_M^O . Proposition 1 closes this gap. Given any observable M , one may obtain the eigenbasis, find another basis that is mutually unbiased with respect to this eigenbasis, and construct C_M^O . An overview of how to construct mutually unbiased bases can be found in [97]. Note that mutually unbiased bases are not the only kinds of bases satisfying Theorem 3.

I now consider the reverse construction. Suppose instead of starting from a given observable M and inferring the basis for the coherence measure, I wish to begin with some basis $\{|i\rangle\}$ and construct an observable M with corresponding measure C_M^O that quantifies the coherence in the basis $\{|i\rangle\}$. The method to do this also follows from Theorem 3, as I can choose any Hermitian matrix to be M so long as the leading diagonals are zero. This is guaranteed to lead to a reasonable measure according to Theorem 3. Such a matrix is easy to construct, as any arbitrary Hermitian matrix written in the basis $\{|i\rangle\}$ with its leading diagonal elements replaced with zero will suffice. This is summarized in the form of the following corollary.

Corollary 3.1. *Consider any complete basis $\{|i\rangle\}$ and any arbitrary Hermitian matrix H which has at least one nonzero off-diagonal element. Then using the matrix $M = H - \sum_i \langle i|H|i\rangle |i\rangle \langle i|$, the corresponding measure C_M^O (See Theorem 3) will always be a measure of the coherence w.r.t. the basis $\{|i\rangle\}$.*

Finally, I show that for MIOs, the corresponding coherence measure

C_M^{MIO} can be written in the form of the semidefinite programming, a sort of linear optimization problem. The form assures the efficiency of computing our measure in terms of the dimension d . Many other quantities related to coherence may be phrased as a semidefinite program. For examples, see [98, 99, 100, 101, 102, 103].

Let us first define the matrix $A := M_A \otimes \rho_B^T \otimes |1\rangle_C \langle 1|$ acting on $\mathcal{H}_A \otimes \mathcal{H}_B \otimes \mathcal{H}_C$. Furthermore, I will assume that $\dim(\mathcal{H}_A) = \dim(\mathcal{H}_B) = d$ and $\dim(\mathcal{H}_C) = 2$.

I now prove the following:

Theorem 4. *For any quantum observable M , the optimization problem*

$$\max_{\Phi \in \text{MIO}} \text{Tr}(M\Phi(\rho))$$

is equivalent to the semidefinite program

$$\begin{aligned} \max_{X \geq 0} \quad & \text{Tr}(AX) \\ \text{subject to} \quad & \text{Tr}_{AC}(X |1\rangle_C \langle 1|) = \mathbb{1}_B \\ & \text{Tr}_{BC}(X \mathbb{1}_A \otimes |i\rangle_B \langle i| \otimes |1\rangle_C \langle 1|) \\ & = \sum_{j=1}^d \text{Tr}_{ABC}(X |j\rangle_A \langle j| \otimes |i\rangle_B \langle i| \otimes |2\rangle_C \langle 2|) |j\rangle_A \langle j| \\ & \forall i = 1, \dots, d, \end{aligned}$$

where $A := M_A \otimes \rho_B^T \otimes |1\rangle_C \langle 1|$.

Note that all the matrices here are assumed to be written in a basis of

the type specified in Theorem 3.

Proof I begin by first noting that the matrix X can be written as the matrix

$$\begin{pmatrix} X_1 & * \\ * & X_2 \end{pmatrix}.$$

The $*$ indicates possible nonzero elements, but they do not appear in the objective function I are trying to optimize, nor do they appear within the linear constraints, so they can be arbitrary so long as $X \geq 0$. The matrix A written in matrix form looks like

$$\begin{pmatrix} M_A \otimes \rho_B^T & 0 \\ 0 & 0 \end{pmatrix}.$$

Computing $\text{Tr}(AX)$, I get

$$\text{Tr}(AX) = \text{Tr}_A[\text{Tr}_B(X_1 \mathbb{1}_A \otimes \rho_B^T) M_A].$$

Now, the constraint $\text{Tr}_{AC}(X |1\rangle_C \langle 1|) = \mathbb{1}_B$ implies $\text{Tr}_A(X_1) = \mathbb{1}_B$, so X_1 actually represents a valid quantum operation in the Choi-Jamiołkowski representation. This implies $\text{Tr}(AX)$ has the form $\text{Tr}_A[\Phi(\rho) M_A]$ for some valid quantum operation Φ .

All that remains is for us to prove that under the set of constraints

$$\begin{aligned} & \text{Tr}_{BC}(X \mathbb{1}_A \otimes |i\rangle_B \langle i| \otimes |1\rangle_C \langle 1|) \\ &= \sum_j \text{Tr}_{ABC}(X |j\rangle_A \langle j| \otimes |i\rangle_B \langle i| \otimes |2\rangle_C \langle 2|) |j\rangle_A \langle j| \end{aligned}$$

for all $i = 1, \dots, d$ and $j = 1, \dots, d$, Φ must be a maximally incoherent operation. I first note that the number $\text{Tr}_{ABC}(X |j\rangle_A \langle j| \otimes |i\rangle_B \langle i| \otimes |2\rangle_C \langle 2|)$ is just the main diagonal elements of the matrix X_2 , so it must be nonnegative since X is positive and X_2 is a principle submatrix of X . I can therefore rewrite the constraint as $\text{Tr}_{BC}(X \mathbb{1}_A \otimes |i\rangle_B \langle i| \otimes |1\rangle_C \langle 1|) = \sum_j \lambda_{i,j} |j\rangle_A \langle j|$ where $\lambda_{i,j}$ is nonnegative. This necessarily means that every incoherent state $|i\rangle \langle i|$ is mapped to a diagonal state $\sum_j \lambda_{i,j} |j\rangle \langle j|$ under the quantum map represented by X_1 , which defines maximally incoherent operations, and completes the proof. ■

3.2.4 Examples

I first provide numerical examples comparing our coherence measures \mathcal{C}_F^M with, a well-known coherence measure, the relative entropy of coherence \mathcal{C}_D [18]. \mathcal{C}_D is defined by $\mathcal{C}_D(\rho) = S(\rho_{\text{diag}}) - S(\rho)$ where $S(\rho) = -\text{Tr} \rho \log \rho$ is the von Neumann entropy of a density matrix ρ and ρ_{diag} is the diagonal part of the density matrix ρ . While \mathcal{C}_F^M requires optimization over all incoherent operations, and the optimal solution for a general quantum state is in general unknown, any incoherent procedure will provide a lower bound for the measure.

I consider the set of m -qubit Dicke state with k excitations. The state is given by

$$|m, k\rangle = \binom{m}{k}^{-\frac{1}{2}} \sum_P |P(\underbrace{0 \dots 0}_{m-k} \underbrace{1 \dots 1}_k)\rangle$$

where P refers to a particular permutation of the state and the summation is over all possible permutations. By verifying the majorization condition

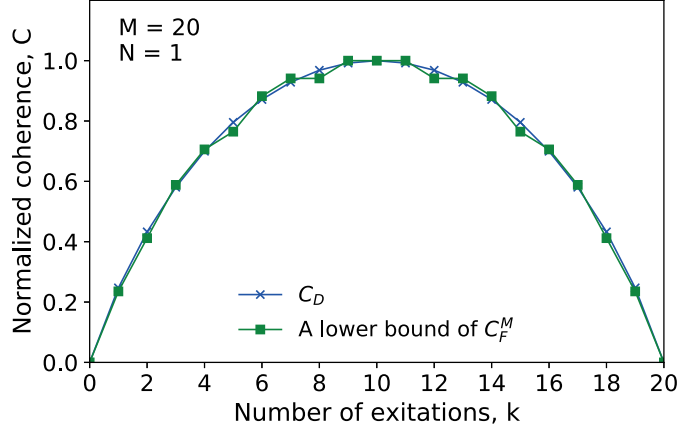


Figure 8: Comparisons between the lower bounds of the superradiant based measure C_S (red, \circ), the QFI based measure C_F^M (green, \square), and the relative entropy of coherence C_R (blue, \times) for the M -qubit Dicke state with k excitations $|M, k\rangle$. The plots are normalized so they coincide at $k = 10$, and demonstrate qualitatively similar behaviour across different measures.

[104] for two uniformly distributed pure states, I can show that there exist incoherent operations Φ which performs the map $|m, n\rangle \xrightarrow{\Phi} (|0\rangle + |1\rangle)^{\otimes m_k}$ where m_k is the largest integer satisfying $2^{m_k} \leq \binom{N}{k}$. I will use this fact to compute a lower bound for C_F^M where $M = m$. For the superradiance based measure, I will simply apply the identity operation. Fig. 8 illustrates the similarity of the obtained lower bounds to the relative entropy of coherence. Note that the computed values are normalized such that they coincide at the point $k = 10$.

Next, I provide numerical example for C_M^Q . Let us consider for spin systems the total magnetic moment operator. For a system of N spins I can choose as our classical basis $\bigotimes_{i=1}^N \{|\uparrow\rangle_i, |\downarrow\rangle_i\}$ where $\{|\uparrow\rangle_i, |\downarrow\rangle_i\}$ is the eigenbasis of the local spin- z operator. In order to witness the coherence between

these basis states, a simple measurement of the magnetization in the x direction will suffice (See Theorem 3 as well as Proposition 1). The total spin- x operator is defined as

$$S_x = \sum_{i=1}^N S_x^i$$

with local spin operators S_x^i . Choosing S_x as our observable, any measurement of $\langle S_x \rangle$ is automatically a lower bound to the corresponding coherence measure $C_{S_x}^O$. Note that because one can equivalently choose to measure the total magnetization along any direction on the equatorial plane, any non zero measurement of $\langle S_x \rangle$ directly implies the presence of coherence in the z direction. Figure 9 compares $C_{l_1} = \sum_{i \neq j} |\rho_{ij}|$, C_D and $C_{S_x}^{\text{MIO}}$ for the state $\rho = (1 + p/7)\mathbb{1}/8 - p/7|w\rangle\langle w|$ where $|w\rangle := \frac{1}{\sqrt{3}}(|001\rangle + |010\rangle + |100\rangle)$ and $p \in [0, 1]$.

3.3 Measuring Nonclassicality via negativity

3.3.1 Nonclassicality filtering

I first introduce the characteristic function of the Glauber-Sudarshan P -function. A common convention is to define it as the integral $\int d^2\alpha P(\alpha) \exp[2i(\beta_i\alpha_r - \beta_r\alpha_i)]$, where α_r, β_r and α_i, β_i are the real and imaginary components of α and β respectively. One observes that this is a multivariate Fourier transformation. For our purposes, I will adopt the following convention:

$$\chi(\beta) := \int d^2\alpha P(\alpha) \exp[2\pi i(\beta_i\alpha_r + \beta_r\alpha_i)].$$

It should be clear that this definition essentially corresponds to a change

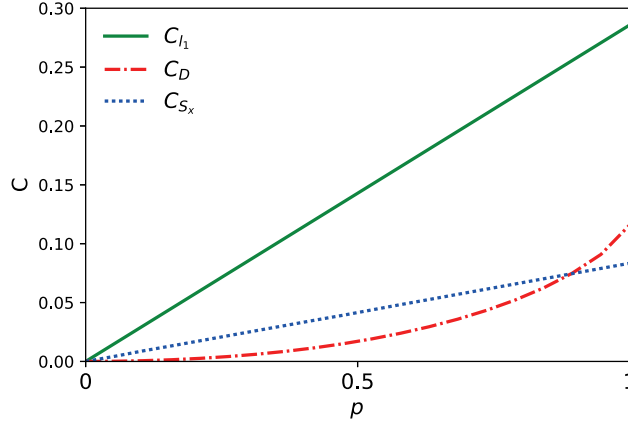


Figure 9: Comparisons among the l_1 norm of coherence C_{l_1} (green, solid), the relative entropy of coherence C_D (red, dash-dotted), and the coherence measure corresponding to magnetization measurement C_{S_x} (blue, dotted). I consider the single parameter, 3 qubit state $\rho = (1 + p/7)\mathbb{1}/8 - p/7|w\rangle\langle w|$, where $|w\rangle := \frac{1}{\sqrt{3}}(|001\rangle + |010\rangle + |100\rangle)$ and $p \in [0, 1]$

in variables of the type $\beta_i \rightarrow \pi\beta'_i$ and $\beta_r \rightarrow -\pi\beta'_r$, and so does not alter the information content of the characteristic function. It also adheres more closely to the conventional definition of the Fourier transform in the ordinary frequency domain: $\mathcal{F}f(y) := \int dx f(x) \exp(-2\pi ixy)$. The corresponding inverse Fourier transform is then $\mathcal{F}^{-1}f(y) := \int dx f(x) \exp(2\pi ixy)$. This allows us to write $P(\alpha) = \mathcal{F}\chi(\alpha)$. All physical characteristic functions satisfies $|\chi(\beta)| \leq \exp(\pi^2|\beta|^2/2)$.

One major issue with the P -function is that it is frequently highly singular. This complicates our ability to analyze and quantify the nonclassicality of quantum states via the P -function alone and necessitates the use of other nonclassicality criteria.

I consider the filtered P -functions proposed in Ref. [105]. Filtered P -

functions are based on the observation that $P(\alpha)$ is the (multivariate) Fourier transform of the characteristic function $\chi(\beta)$, such that $P(\alpha) = \mathcal{F}\chi(\alpha)$. This opens up the possibility of applying a filtering function $\Omega_w(\beta)$ prior to the Fourier transform. The nonnegative parameter w is to be interpreted as the width of the filter. The filtered function is then

$$P_{\Omega,w}(\alpha) := \mathcal{F}\chi_{\Omega,w}(\alpha)$$

where $\chi_{\Omega,w}(\beta) := \chi(\beta)\Omega_w(\beta)$. In general, the characteristic, P and filtered P -functions depend on the state ρ . When the state ρ is unambiguous, the characteristic function is denoted χ and $\chi(\alpha)$ is the function at the point α . When ρ needs to be specified, the characteristic function is denoted $\chi(\rho)$, while $\chi(\alpha | \rho)$ is the function at α . Similar notations will also be used for the unfiltered and filtered P -functions. The goal is to be able to consistently define the negativity of the P -function, even when it is highly singular. For this purpose, I consider a carefully chosen nonclassicality filter Ω_w satisfying the following properties:

- (a) $\Omega_w(\beta)$ is factorizable such that $\Omega_w(\beta) = \Omega_w^1(\beta)\Omega_w^2(\beta)$ s.t. $\Omega_w^i(\beta)$ is square integrable for $i = 1, 2$.
- (b) $\Omega_w^1(\beta)e^{\pi^2|\beta|^2/2}$ is square integrable.
- (c) $\Omega_w(0) = 1$ and $\lim_{w \rightarrow \infty} \Omega_w(\beta) = 1$.
- (d) There exists $t > 0$ such that $\Omega_w(\beta) = \Omega_{w/|r|}(\beta)\Omega_t(\beta)$ for any $|r| < 1$, and some $t > 0$.

(e) $\Omega_w(\beta) = \Omega_{kw}(k\beta)$ for any $k > 0$.

Note that these conditions are stronger than those proposed in Ref. [105]. There, the key requirement is for $\Omega_w(\beta)e^{\pi^2|\beta|^2/2}$ to be square-integrable, in order to ensure that its Fourier transform will also be square-integrable due to Plancherel's theorem. Square integrability is however not sufficient to ensure that $P_{\Omega,w}(\alpha)$ is pointwise finite for every α . Our modified approach closes this gap by ensuring that $P_{\Omega,w}(\alpha)$ is always finite, which allows us to numerically determine whether there is negativity at a given point α .

Theorem 5. *If Ω_w satisfies properties (a) and (b), then $P_{\Omega,w}(\alpha)$ contains no singularities and is finite for every α .*

Proof Since $\chi_{\Omega,w}(\beta) \equiv \chi(\beta)\Omega_w(\beta) = \chi(\beta)\Omega_w^1(\beta)\Omega_w^2(\beta)$, I can group the terms such that $\chi_{\Omega,w}(\beta) = [\chi(\beta)\Omega_w^1(\beta)] \times \Omega_w^2(\beta)$. The convolution theorem then implies that $P_{\Omega,w}(\alpha) \equiv \mathcal{F}\chi_{\Omega,w}(\alpha) = \{\mathcal{F}[\chi(\beta)\Omega_w^1(\beta)] * \mathcal{F}\Omega_w^2(\beta)\}(\alpha)$.

From property (a), I already know that $\Omega_w^2(\beta)$ and hence $\mathcal{F}\Omega_w^2(\beta)$ are square integrable from Plancherel's theorem. Furthermore, from property (b), I am guaranteed that $\Omega_w^1(\beta)e^{\pi^2|\beta|^2}$ is square integrable. This means that $\Omega_w^1(\beta)\chi(\beta)$ is also square integrable since $\chi(\beta) \leq e^{\pi^2|\beta|^2}$. Applying Plancherel's theorem again, I know that $\mathcal{F}[\chi(\beta)\Omega_w^1(\beta)]$ is also square integrable.

I recall that if $f(\beta)$ and $g(\beta)$ are both square integrable, then by Cauchy's inequality, it must satisfy $\|f(\beta)g(\beta)\|_1 \leq \|f(\beta)\|_2\|g(\beta)\|_2$ where $\|\cdot\|_1$ and $\|\cdot\|_2$ are the L_1 and L_2 norms respectively. Furthermore, since the L_1 norm is just the absolute integral, I have

$$\left| \int d^2\beta f(\beta)g(\beta) \right| \leq \|f(\beta)\|_2\|g(\beta)\|_2 < \infty.$$

This implies that the integral $\int d^2\beta f(\beta)g(\beta)$ is finite.

$\{\mathcal{F}[\chi(\beta)\Omega_w^1(\beta)] * \mathcal{F}\Omega_w^2(\beta)\}(\alpha)$ is a convolution of two square integrable functions. By the definition of a convolution, for every given α , it is an integral of a product of 2 square integrable functions. From the property described in the previous paragraph, I must have $P_{\Omega,w}(\alpha) \equiv \mathcal{F}\chi_{\Omega,w}(\alpha) = \{\mathcal{F}[\chi(\beta)\Omega_w^1(\beta)] * \mathcal{F}\Omega_w^2(\beta)\}(\alpha) < \infty$, so it has a finite value for every α . This means that the filtered function $P_{\Omega,w}(\alpha)$ is finite everywhere and contains no singularities. ■

Theorem 5 thus allows us to assign definite positive or negative values at every point α of $P_{\Omega,w}(\alpha)$. This implies that I can determine unambiguously the positive and negative regions of $P_{\Omega,w}(\alpha)$ as follows:

Definition 2 (Negativity of a P function). *Let $f(\alpha)$ be a function that is well defined for every α , so that I can write $f(\alpha) = f^+(\alpha) - f^-(\alpha)$, where $f^\pm(\alpha)$ are pointwise nonnegative functions. Then the negativity of f is defined as*

$$\mathcal{N}(f) := \int d^2\alpha f^-(\alpha).$$

Consider the P function of a state ρ . Let Ω_w be some filter that satisfies properties (a)-(c). I can then write the filtered P -function as $P_{\Omega,w}(\alpha) = P_{\Omega,w}^+(\alpha) - P_{\Omega,w}^-(\alpha)$ where $P_{\Omega,w}^\pm(\alpha)$ are the nonnegative functions.

The negativity, of ρ is defined to be

$$\mathcal{N}(\rho) := \lim_{w \rightarrow \infty} \int d^2\alpha P_{\Omega,w}^-(\alpha).$$

Property (c) then guarantees that the filtered function is a proper quasiprob-

ability function such that $\int d^2\alpha P_{\Omega,w}(\alpha) = 1$, and that for sufficiently large w , $\mathcal{F}\Omega_w(\alpha) \approx \delta(\alpha)$, so the original P -function is retrieved.

Given the above definitions, one still needs to find an appropriate filter Ω_w . The astute reader may have noticed that properties (d) and (e) are not yet discussed. They will play an important role which will be described in greater detail in a subsequent section. I first establish several properties of the negativity.

3.3.2 Negativity as a linear optical monotone

In Ref. [74], a resource theoretical approach was proposed to quantify nonclassicality in radiation fields. There, it was argued that nonclassicality measures should be linear optical monotones, i.e. nonclassicality should be measured using quantities that do not increase under linear optical maps. Under this approach, nonclassicality may be considered as a resource that overcomes the limitations of linear optics.

Linear optical maps are formally defined to be any quantum map that can be written in the form

$$\Phi_L(\rho_A) := \text{Tr}_E[U_L(\rho_A \otimes \sigma_E)U_L^\dagger],$$

where σ_E is a classical state and U_L is a linear optical unitary composed of any combination of beam splitters, phase shifters and displacement operations. Such unitary transforms will always map a N mode bosonic creation operator $a_\mu^\dagger := \sum_{i=1}^N \mu_i a_i^\dagger$ into $a_{\vec{\mu}}^\dagger + \oplus_{i=1}^N \alpha_i \mathbb{1}_i$ where $\vec{\mu}, \vec{\mu}'$ are N dimensional complex vectors of unit length, and $\mathbb{1}_i$ is the identity operator on the i th

mode.

One may also incorporate postselection into the definition by defining selective linear optical operations via a set of Kraus operators K_i for which there exists linear optical unitary U_L , classical ancilla $\sigma_{EE'}$, and a set of orthogonal vectors $\{|i\rangle_{E'}\}$ such that $\text{Tr}_E[U_L(\rho_A \otimes \sigma_{EE'})U_L^\dagger] = \sum_i p_i \rho_A^i \otimes |i\rangle_{E'}\langle i|$, where $p_i \rho_A^i := K_i \rho_A K_i^\dagger$ and $p_i := \text{Tr}(K_i \rho_A K_i^\dagger)$.

Based on this definition, the following theorem shows that the negativity \mathcal{N} forms a linear optical monotone that belongs to the operational resource theory outlined in Ref. [74].

Theorem 6. *The negativity $\mathcal{N}(\rho)$ is a nonclassicality measure satisfying the following properties:*

1. $\mathcal{N}(\rho) = 0$ if and only if ρ has a classical P -function.
2. (a) (Weak monotonicity) $\mathcal{N}(\rho) \geq \mathcal{N}(\Phi_L(\rho))$.
(b) (Strong monotonicity) $\mathcal{N}(\rho) \geq \sum_i p_i \mathcal{N}(\rho_i)$ where $p_i := \text{Tr}(K_i^\dagger K_i \rho)$, $\rho_i := (K_i \rho K_i^\dagger)/p_i$ and $\Phi_L(\rho) = \sum_i K_i \rho K_i^\dagger$ is a selective linear optical operation.
3. (Convexity), i.e. $\mathcal{N}(\sum_i p_i \rho_i) \leq \sum_i p_i \mathcal{N}(\rho_i)$.

Proof It is apparent that if the P -function of ρ is classical, then $\mathcal{N}(\rho) = 0$ since $P_{\Omega,w}(\alpha) \rightarrow P(\alpha)$ as $w \rightarrow \infty$ so the negative volume must vanish. The converse must also be true as if $\mathcal{N}(\rho) = 0$, then $\int d^2\alpha P_{\Omega,w}^-(\alpha) \rightarrow 0$ as $w \rightarrow \infty$, which implies $P_{\Omega,w}^+(\alpha) \rightarrow P(\alpha)$. This means that $P(\alpha)$ is the limit of a sequence of positive distributions. As the set of classical states is a closed

convex set, and $P_{\Omega,w}^+(\alpha) \rightarrow P(\alpha)$, this means that $P(\alpha)$ must be classical. This proves Property 1.

In order to prove the weak and strong monotonicity properties, I make use of an observation from Ref [74]. It was noted that for the special case when the P is any regular function that does not contain any singularities, the negative volume $\mathcal{N}(\rho)$ where $\rho = \int d^2\alpha P(\alpha) |\alpha\rangle\langle\alpha|$ satisfies both weak and strong monotonicity conditions.

I now extend the above result to all P functions. Let

$$\rho_w = \int d^2\alpha P_{\Omega,w}(\alpha) |\alpha\rangle\langle\alpha|.$$

For weak monotonicity, I see that $\mathcal{N}(\rho_w) \geq \mathcal{N}(\Phi_L(\rho_w))$. Taking the limit $w \rightarrow \infty$, $\rho_w \rightarrow \rho$, the inequality converges to $\mathcal{N}(\rho) \geq \mathcal{N}(\Phi_L(\rho))$. Identical arguments hold for strong monotonicity. This is sufficient to generalize the monotonicity property to all P functions, and establishes Property 2.

Similarly for convexity, I have $\mathcal{N}(\sum_i p_i \rho_{w,i}) \leq \sum_i p_i \mathcal{N}(\rho_{w,i})$ for every w . Taking the limit $w \rightarrow \infty$, $\rho_{w,i} \rightarrow \rho_i$ so the inequality converges to $\mathcal{N}(\sum_i p_i \rho_i) \leq \sum_i p_i \mathcal{N}(\rho_i)$ which is the required inequality.

■

3.3.3 Operational interpretations of the negativity

An operational measure that has been extensively studied in various quantum resource theories is the robustness[106, 98]. It quantifies the minimum amount of mixing with noise that is necessary to make a given quantum state classical. It turns out that the negativity exactly quantifies the ro-

bustness of a given quantum state.

I can consider the following definition for the robustness of nonclassicality.

Definition 3 (Robustness of nonclassicality). *Let \mathcal{P} be the set of all quantum states with classical P distributions.*

The robustness of nonclassicality is defined as

$$\mathcal{R}(\rho) := \min_{\sigma \in \mathcal{P}} \{r \mid r \geq 0, \frac{\rho + r\sigma}{1+r} \in \mathcal{P}\}.$$

Based on the above definition, one may show that the negativity and the robustness are in fact equivalent.

Theorem 7. *The negativity and the robustness are equivalent measures of nonclassicality, i.e. $\mathcal{N}(\rho) = \mathcal{R}(\rho)$ for every quantum state ρ .*

Proof

First, note that I can always write $P_{\Omega,w}(\alpha) = P_{\Omega,w}^+(\alpha) - P_{\Omega,w}^-(\alpha)$ where $P_{\Omega,w}^\pm(\alpha)$ are pointwise nonnegative functions. Let $\int d^2\alpha P_{\Omega,w}^-(\alpha) := r_w$ and $\lim_{w \rightarrow \infty} r_w = r$. Note that by this definition, $r = \mathcal{N}(\rho)$

I now consider some sufficiently large w and observe that r is always an upper bound to the robustness. This is because, $\frac{1}{1+r_w}(P_{\Omega,w}(\alpha) + P_{\Omega,w}^-(\alpha)) = \frac{1}{1+r_w}P_{\Omega,w}^+(\alpha)$ which corresponds to a positive, and hence classical, P -function. Therefore, if ρ_w and σ_w are the quantum states corresponding to the distributions $P_{\Omega,w}(\alpha)$ and $P_{\Omega,w}^-(\alpha)/r_w$ respectively, the mixture $\frac{\rho_w + r_w\sigma_w}{1+r_w}$ always has a classical P -function. Taking the limit $w \rightarrow \infty$, I get $\frac{\rho + r\sigma}{1+r}$ is classical, where $\sigma := \lim_{w \rightarrow \infty} \sigma_w$. Since r is just the negativity $\mathcal{N}(\rho)$, I see that the

negativity is at least an upper bound to the robustness.

I now need to show that r is also a lower bound. This follows immediately from the observation that $P_{\Omega,w}^-(\alpha)$ is the minimal function necessary for $P_{\Omega,w}(\alpha)$ to be positive. It is clear that if $P'(\alpha) < P_{\Omega,w}^-(\alpha)$ for any α , then $P_{\Omega,w}(\alpha) + P'(\alpha) < 0$ and so is not positive at α . This shows that r must also be a lower bound and proves the theorem.

■

Theorem 7 therefore provides a direct operational interpretation for the negativity of the P -function. The negativities of other s -parametrized quasiprobabilities can then be interpreted as lower bounds to the robustness. I also point out that $P_s(\alpha)$ may be interpreted as the P -function after interaction with a thermal environment[107, 108, 109]. This means that at $s < 1$, the negativity corresponds to the robustness of the state under less than ideal environmental conditions, while at $s = 1$, it is the robustness under ideal conditions.

Another possible interpretation of the negativity is the cost of simulating a nonclassical state in phase space using P function. In particular, it is possible to show that the number of samples $s(\epsilon, \delta)$ required to classically simulate the measurement outcomes with a sampling error less than ϵ and success probability greater than $1 - \delta$ scales with[110]

$$s(\epsilon, \delta) \propto [1 + 2\mathcal{N}(\rho)]^2.$$

As $\mathcal{N}(\rho) = 0$ when the state is classical, the factor $[1 + 2\mathcal{N}(\rho)]^2$ describes the additional overhead required to simulate a nonclassical state.

This suggests that states with greater negativities tend to be harder to simulate.

3.3.4 Approximate nonclassicality monotones

The negativity is well defined in Definition 2, but does not always lead to finite quantities. For instance, highly singular states such as squeezed states can possess infinite negativities. This can be verified numerically by applying an appropriate filter and computing the filtered negativities as $w \rightarrow \infty$. From Theorem 7, I know that this is because some states require an infinite amount of statistical mixing with classical states before their nonclassicality is erased. Nevertheless, \mathcal{N} remains a linear optical monotone, which is able to unambiguously identify every nonclassical state.

It is natural to ask whether it is possible to avoid infinite values while simultaneously maximizing the number of identifiable nonclassical states. I show that this is possible via an appropriate choice of filters that satisfies the full suite of properties (a)-(e) (see Preliminaries).

Theorem 8. *If the filter Ω_w satisfies properties (a)-(e), with $\delta := \mathcal{N}(\mathcal{F}\Omega_{w=1})$, the filtered negativity $\mathcal{N}(P_{\Omega,w})$ is an approximate nonclassicality measure satisfying the following properties:*

1. $\mathcal{N}(P_{\Omega,w}) \leq \delta$ if ρ is classical.
2. (Approximate monotonicity) For any linear optical map Φ_L , $(1 + 2\delta)\mathcal{N}[P_{\Omega,w}(\rho)] + \delta \geq \mathcal{N}\{P_{\Omega,w}[\Phi_L(\rho)]\}$.
3. (Convexity) $\mathcal{N}[P_{\Omega,w}(\sum_i p_i \rho_i)] \leq \sum_i p_i \mathcal{N}[P_{\Omega,w}(\rho_i)]$

Lemma 2. Suppose f and g are non-singular real-valued functions on the complex plane \mathbb{C} such that $\int d^2\alpha f(\alpha) = \int d^2\alpha g(\alpha) = 1$. Then,

$$\mathcal{N}(f * g) \leq \mathcal{N}(f)(1 + 2\mathcal{N}(g)) + \mathcal{N}(g)$$

Proof

Let $f(\alpha) = f^+(\alpha) - f^-(\alpha)$, and $g(\alpha) = g^+(\alpha) - g^-(\alpha)$, where $f^\pm(\alpha)$ and $g^\pm(\alpha)$ are pointwise nonnegative functions. I note that $f * g = (f^+ - f^-) * (g^+ - g^-) = f^+ * g^+ + f^- * g^- - (f^+ * g^- + f^- * g^+)$. As a result, I have the following series of inequalities

$$\begin{aligned} & \int d^2\alpha (f * g)^-(\alpha) \\ & \leq \int d^2\alpha (f^+ * g^-(\alpha) + f^- * g^+(\alpha)) \\ & = \int d^2\alpha f^+(\alpha) \int d^2\alpha g^-(\alpha) + \int d^2\alpha f^-(\alpha) \int d^2\alpha g^+(\alpha) \\ & = (1 + \int d^2\alpha f^-(\alpha)) \int d^2\alpha g^-(\alpha) \\ & \quad + \int d^2\alpha f^-(\alpha) (1 + \int d^2\alpha g^-(\alpha)) \\ & = \int d^2\alpha g^-(\alpha) (1 + 2 \int d^2\alpha f^-(\alpha)) + \int d^2\alpha f^-(\alpha), \end{aligned}$$

where I used the identity $\int d^2\alpha f^+(\alpha) = 1 + \int d^2\alpha f^-(\alpha)$ which comes from the fact that $\int d^2\alpha f(\alpha) = 1$.

■

Lemma 3. Suppose the filter Ω_w satisfies property (a)-(c) and (e). Then for any given linear optical map Φ_L , $\mathcal{N}[P_{\Omega,w}(\rho)] \geq \mathcal{N}\{P_{\Omega,w/|r|}[\Phi_L(\rho)]\}$ where

the factor r depends only on Φ_L .

Proof

Similar to an observation from Ref. [109] and the proof of Theorem 6, I define the map

$$\Phi_{\Omega,w}(\rho) = \int d^2\gamma \mathcal{F}\Omega_w(\gamma) D(\gamma) \rho D^\dagger(\gamma).$$

From this, I see that $P(\Phi_{\Omega,w}(\rho)) = P_{\Omega,w}(\rho)$, so the P -function after this map is equivalent to applying a filter Ω_w . This property does not require $\mathcal{F}\Omega_w(\alpha)$ to be pointwise positive for every α .

Using the notation $\mathcal{D}_\alpha(\cdot) = D(\alpha)(\cdot)D^\dagger(\alpha)$, I follow a similar argument with the proof of Theorem 6, resulting in the following series of inequalities:

$$\mathcal{N}[\Phi_{\Omega,w}(\rho)] \geq \mathcal{N}[\Phi_L \Phi_{\Omega,w}(\rho)] \quad (3.2)$$

$$= \mathcal{N}[\Phi_L \int d^2\alpha \mathcal{F}\Omega_w(\alpha) \mathcal{D}_\alpha(\rho)] \quad (3.3)$$

$$= \mathcal{N}[\int d^2\alpha \mathcal{F}\Omega_w(\alpha) \mathcal{D}_{|r|\alpha} \Phi_L(\rho)] \quad (3.4)$$

$$= \mathcal{N}[\int \frac{d^2\alpha}{|r|^2} \mathcal{F}\Omega_w(\frac{\alpha}{|r|}) \mathcal{D}_\alpha \Phi_L(\rho)] \quad (3.5)$$

$$= \mathcal{N}(\int d^2\alpha \mathcal{F}\Omega_{w/|r|}(\alpha) \mathcal{D}_\alpha \Phi_L(\rho)) \quad (3.6)$$

$$= \mathcal{N}(\Phi_{\Omega,w/|r|} \Phi_L(\rho)), \quad (3.7)$$

where $|r| \leq 1$ and depends only on Φ_L . Which is the required expression.

Eqn. 3.6 comes from the observation that whenever the filter satisfies $\Omega_w(\beta) = \Omega_{kw}(k\beta)$ for any $k > 0$ (property (e)), then together with the scaling property

$\mathcal{F}[f(|r|\beta)](\alpha) = \mathcal{F}f(\alpha/|r|)/|r|^2$ I have

$$\mathcal{F}\Omega_w(\alpha/|r|) = |r|^2 \mathcal{F}\Omega_{w/|r|}(\alpha).$$

■

Theorem 8 suggests that given a filter that satisfies properties (a)-(e), the filtered negativity $\mathcal{N}_{\Omega,w}(\rho)$ is an approximate linear optical monotone when the negativity of $\mathcal{F}\Omega_w$ is small. Ideally, I would like the Fourier transform of the filter to be pointwise positive and still satisfy properties (a)-(e), which would imply that the filtered negativity is an exact linear optical monotone that can be computed for every $w > 0$. It remains unclear whether this is possible, but I demonstrate that the negativity of the filter can at least be made arbitrarily small, such that the filtered negativity is essentially a linear optical monotone to any required level of precision.

Proposition 2. Define $\Omega_{w,\varepsilon}(\beta) := \exp(-|\beta/w|^{2+\varepsilon})$, where $w > 0$ is the width parameter, and $\varepsilon > 0$ is the error parameter. Then, $\Omega_{w,\varepsilon}$ is a filter that satisfies properties (a)-(e). Furthermore, $\mathcal{N}(\mathcal{F}\Omega_{w=1,\varepsilon}) \rightarrow 0$ as $\varepsilon \rightarrow 0$.

Proof

Consider any given linear optical map Φ_L . By Lemma 2, for a state $\Phi_L(\rho)$, I obtain

$$\begin{aligned} & \mathcal{N}\{P_{\Omega,w}[\Phi_L(\rho)]\} \\ & \leq \mathcal{N}\{P_{\Omega,w/|r|}[\Phi_L(\rho)]\}[1 + 2\mathcal{N}(\mathcal{F}\Omega_t)] + \mathcal{N}(\mathcal{F}\Omega_t) \end{aligned}$$

Combining the above and Lemma 3, I get the following inequalities:

$$\begin{aligned}\mathcal{N}[P_{\Omega,w}(\rho)] &\geq \mathcal{N}\{P_{\Omega,w/|r|}[\Phi_L(\rho)]\} \\ &\geq \frac{\mathcal{N}\{P_{\Omega,w}[\Phi_L(\rho)]\} - \mathcal{N}(\mathcal{F}\Omega_t)}{1 + 2N(\mathcal{F}\Omega_t)}\end{aligned}$$

Define $\delta = N(\mathcal{F}\Omega_t)$.

Finally, I observe that because $\Omega_w(\alpha) = \Omega_{kw}(k\alpha)$ for any $k > 0$, if I set $w = 1$ and $k = t$, I get $\Omega_{w=1}(\alpha) = \Omega_t(t\alpha)$. From the scaling property of the Fourier transform $\mathcal{F}[\Omega_t(t\beta)](\alpha) = \mathcal{F}\Omega_t(\alpha/t)/t^2$, I also have that $\int d^2\alpha \mathcal{F}\Omega_t^-(\alpha/t)/t^2 = \int d^2\alpha \mathcal{F}\Omega_t^-(\alpha)t^2/t^2 = \mathcal{N}(\mathcal{F}\Omega_t)$. This implies that $\mathcal{N}(\mathcal{F}\Omega_{w=1}) = \mathcal{N}(\mathcal{F}\Omega_t)$ for any $t > 0$, which completes the proof. ■

3.3.5 Examples

Here, I provide some numerical examples that illustrates our results for the negativity of the P -function \mathcal{N} and the filtered negativity $\mathcal{N}_{\Omega,w} := \mathcal{N}(P_{\Omega,w})$ using several prominent nonclassical states. I will use the filter $\Omega_{w,\varepsilon}$ from Proposition 2. The error parameter ε is chosen to be $\varepsilon = 0.21$ such that $2\delta = 2\mathcal{N}(\Omega_{w=1,\varepsilon}) \approx 0.05$. From Theorem 8, this means that the resulting filtered negativity $\mathcal{N}_{\Omega,w}$ is a linear optical monotone up to approximately a 5 percent error. Note that this choice is arbitrary, as δ can be made as small as desired by decreasing ε .

For highly nonclassical states such as Fock and squeezed-vacuum states \mathcal{N} is infinitely large, which can be verified numerically via Definition 2. One example of a nonclassical state with finite \mathcal{N} is the single-photon-added thermal (SPAT) state, defined by $\rho_{\text{SPAT}} = a^\dagger e^{-\beta\hbar\omega a^\dagger a} / \text{Tr}(e^{-\beta\hbar\omega a^\dagger a} a a^\dagger)$. Its

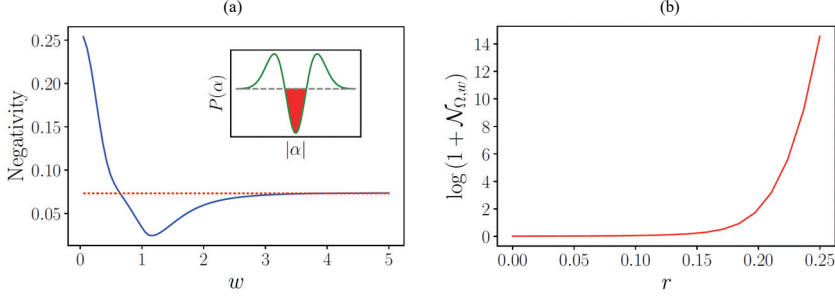


Figure 10: (a) Convergence of the filtered negativity (solid line) $\mathcal{N}_{\Omega,w}$ to the negativity (dotted line) \mathcal{N} for the single photon added thermal state ρ_{SPAT} with $\bar{n} = 2$. (b) The (logged) filtered negativity $\log(1 + \mathcal{N}_{\Omega,w})$ for squeezed vacuum $|r\rangle$.

characteristic function is $\chi_{\text{SPAT}}(\beta) = [1 - \pi^2(1 + \bar{n})|\beta|^2]e^{-\pi^2|\beta|^2/\bar{n}}$, and the corresponding P -function is $P_{\text{SPAT}}(\alpha) = \frac{1+\bar{n}}{\pi\bar{n}^3} \left(|\alpha|^2 - \frac{\bar{n}}{1+\bar{n}} \right) e^{-|\alpha|^2/\bar{n}}$ [111]. Figure 10 (a), illustrates how the the filtered negativity $\mathcal{N}_{\Omega,w}(\rho_{\text{SPAT}})$ approaches $\mathcal{N}(\rho_{\text{SPAT}})$ as $w \rightarrow \infty$, which comes directly from Definition 2. From Theorem 6, I know that the negativity $\mathcal{N}(\rho_{\text{SPAT}})$ cannot be increased via linear optical processes.

The negativity can be infinite in general. One example is the squeezed vacuum state $|r\rangle = e^{r(a^{\dagger 2} - a^2)/2} |0\rangle$. Its characteristic function is $\chi_{|r\rangle}(\beta = x + iy) = \exp\left\{ \frac{\pi^2}{2} [(s - e^{2r})x^2 + (s - e^{-2r})y^2] \right\}$ for $r > 0$. The Wigner function ($s = 0$) is Gaussian, so it does not show any negative value. However, its P function ($s = 1$) shows extremely singular behavior, and one can numerically verify that \mathcal{N} is infinite. This can be circumvented by considering the filtered negativity $\mathcal{N}_{\Omega,w}$.

Figure 10 illustrates the filtered negativities $\mathcal{N}_{\Omega,w}$ of the squeezed vacuum states $|r\rangle$ with squeezing parameter r . I see that the filtered negativ-

ity captures the increase in nonclassicality due to the increase in squeezing r . As the filter $\Omega_{w,\varepsilon}$ has non-zero negativity, $\mathcal{N}_{\Omega,w}$ is only an approximate monotone (see Theorem 8), but this error can be made arbitrarily small by decreasing the parameter ε . This may, however, require increased numerical precision and hence incur additional computational costs.

3.4 Remarks

In the preceding sections, I have demonstrated how to construct, via quantum Fisher information, valid measures of quantum coherence. It was in fact already known that some form of coherence plays a crucial role in quantum metrology. In [112], it was pointed out that *unspeakable* coherence is especially relevant for metrology, and that the resource theory of asymmetry is able to quantify the metrological usefulness of a given probe state. Our results, in the form of Thms. 1 goes one step further, by demonstrating that more general forms of coherence may in fact be made useful via an appropriate incoherent operation. In contrast, an operation such as the type considered in Lemma 1 is explicitly forbidden in theories of asymmetry.

Furthermore, I demonstrated that every nontrivial Hermitian observable M corresponds to a coherence witness and a coherence measure C_M^O for some specific incoherent bases, where the set of operations O may be either MIO or IO. In the case of MIO, I show that the measure is always computable via a semidefinite program, leading to an infinitely large set of computable coherence measures. The measures also show that the task of optimizing $\langle M \rangle$ is the same as the task of maximizing the coherence of the

input state, up to the application of some incoherent operation (Theorem 3). They, therefore, have the operational interpretation of the usefulness of a given quantum state ρ for the purpose of optimizing the mean value of the observable $\langle M \rangle$.

A key conclusion of our results, in particular Theorem 3, is that every nontrivial quantum observable corresponds to a computable coherence measure, which also implies that every such quantum observable is also a coherence witness. This may in some cases allow coherence to be verified in the laboratory using simpler measurements, which was discussed in Section 3.2.4. In spin systems, for example, a magnetization measurement is sufficient and relatively simpler to implement over a mathematically optimal measurement [113]. Moreover, the measurement outcomes of such observables are always, up to a constant displacement, a lower bound to a corresponding coherence measure C_M^O .

For the nonclassicality, I introduced a method to define the negativity of the s -parametrized quasiprobabilities. Our method is based on a modified version of the filtered P -function in Ref.[105]. Based on this definition, it is possible to show that the negativity of the set of s -parametrized quasiprobabilities are all linear optical monotones, and form a continuous hierarchy of increasingly weaker nonclassicality measures that all belong to the operational resource theory of nonclassicality considered in Refs. [74, 21].

In general, the negativity may have infinite values. In order to circumvent this, I introduce an approximate linear optical monotone that is finite computable and able to identify nearly every nonclassical state. A key advantage of this approach is that the set of unidentifiable nonclassical states

can be made to converge by increasing the parameter w . The error can also be controlled via a single parameter ϵ .

I also demonstrate in Theorem 7 that the negativity of the P -function has a direct operational interpretation as the robustness. Since $\mathcal{N}(\rho)$ is not always finite, this means that there are some states whose nonclassicality cannot be erased by simple statistical mixing with classical noise. This is a characteristic it shares with quantum coherence, where simple mixing with an incoherent state cannot make the state classical in general [98].

The following is the publication list related to this chapter:

1. K. C. Tan, S. Choi, H. Kwon, and H. Jeong, "Coherence, quantum Fisher information, superradiance, and entanglement as interconvertible resources," *Phys. Rev. A* 97, 052304 (2018).
2. K. C. Tan, S. Choi, and H. Jeong, "Optimizing nontrivial quantum observables using coherence," *New J. Phys.* 21, 023013 (2019).
3. K. C. Tan, S. Choi, and H. Jeong, "Negativity of Quasiprobability Distributions as a Measure of Nonclassicality," *Phys. Rev. Lett.* 124, 110404 (2020).] [114].

Chapter 4

Conclusion

In optical quantum information processing, the entanglement and other quantum resources are distinctive features of quantum optics that overcome the classical limitation. One of the prominent protocol using the entanglement is teleportation [5]. Especially, one can use teleportation to send quantum information in an optical qubit robustly under the photon loss [115]. The efficiency of the teleportation, however, depends on the qubit encoding. One objective of this dissertation is to analyze the hybrid entanglement between two different encodings to combine their respective merits. Furthermore, other quantum resources that optical systems may have investigated by the resource theoretic framework. The resource theories of coherence and nonclassicality are such kind. In this context, I have focused on providing operational measures about these quantum characteristics that manifest the relations with other physical phenomena or operational tasks.

Regarding the teleportation with the hybrid entanglement, I have considered the hybrid entangled states of a many-photon qubit and a small-photon qubit. The many-photon qubit encodings have merit on the success probability of the Bell-state measurement, and the small-photon qubit encodings have on loss tolerance. First, I have analyzed the teleportation using the hybrid entangled state between a coherent-state qubit and VSP qubit. Here, the coherent-state qubit with large amplitude serves as a many-photon

qubit. The success probability depends only on the coherent-state qubit and increases as the amplitude of the coherent-state qubit is larger. Whereas, the fidelity depends on both loss rates. It has been shown that the loss on the coherent-state qubit more severely reduces the fidelity than on the VSP qubit. In this case, the hybrid entanglement helps the fidelity from decreasing by balancing these two loss rates.

Second, I have considered the entanglement between a multiphoton-qubit and a small-photon qubit. The candidates for the small-photon qubit are the coherent-state qubit with a small amplitude, the PSP qubit, and the VSP qubit. In contrast with the previous case, the fidelity of the output state depends only on the loss of the sent small-photon qubit of the hybrid entangled state. Among the candidates, the VSP qubit shows the generally best fidelity. However, since the VSP qubit has weakness on single-qubit operations one should manifest the context of usage. From the fact that the success probability is independent of the loss on the small-photon qubit, I conclude that the multiphoton qubit compensates for the weakness of each qubit by the hybrid approach. The generation methods of the required hybrid entangled states have been discussed.

For the resource theoretic quantification of the quantumness of the optical system, I have considered the resource theory of coherence and that of nonclassicality. First, I have proved the coherence measures driven from the quantum Fisher information and quantum observables are genuine measures satisfying the conditions such as faithfulness, strong and weak monotonicity, and convexity. The former measure for a pure state is defined as the maximization of the sum of the quantum Fisher information under incoher-

ent operations where a state is distributed over N parties and each one has a local signal Hamiltonian whose eigenstates forms the incoherent basis. The general mixed is constructed by the convex roof. The latter observable coherent measure also has the optimization over the maximally incoherent operation, but I have shown that the maximization can be computed by the semidefinite programming.

Our nonclassicality measure is defined as the negativity of the P function. The negativity of the P function has been known as the linear optical monotone only for states having the regular P function. In our study, however, I have used the filtering so that the negativity is well-defined (including the positive infinity) even for the singular P function. Furthermore, have shown that our measure captures the robustness on the mixing with classical states, which gives its operational meaning. The definition of the measure contains the limit on the filtering parameter, but I have proved that even for the finite filtering, the measure still has the monotonicity on the linear optical map.

Our work may be useful for the optical realization of long-distance quantum information processing by exploring hybrid architectures of optical networks. I also hope that our study may help the further understanding of the quantumness of the optical system.

Bibliography

- [1] C. H. Bennett and G. Brassard, “Quantum cryptography: Public key distribution and coin tossing,” Theoretical Computer Science, vol. 560, pp. 7 – 11, 2014.
- [2] P. W. Shor, “Algorithms for quantum computation: discrete logarithms and factoring,” in Proceedings 35th Annual Symposium on Foundations of Computer Science, pp. 124–134, 1994.
- [3] L. K. Grover, “A fast quantum mechanical algorithm for database search,” in Proceedings 28th Annual ACM Symposium on the Theory of Computing, pp. 212–219, 1996.
- [4] S. L. Braunstein and C. M. Caves, “Statistical distance and the geometry of quantum states,” Physical Review Letters, vol. 72, pp. 3439–3443, 1994.
- [5] C. H. Bennett, G. Brassard, C. Crépeau, R. Jozsa, A. Peres, and W. K. Wootters, “Teleporting an unknown quantum state via dual classical and einstein-podolsky-rosen channels,” Physical Review Letters, vol. 70, pp. 1895–1899, 1993.
- [6] S. Pirandola, J. Eisert, C. Weedbrook, A. Furusawa, and S. L. Braunstein, “Advances in quantum teleportation,” Nature Photonics, vol. 9, no. 10, pp. 641–652, 2015.
- [7] S. Wehner, D. Elkouss, and R. Hanson, “Quantum internet: A vision for the road ahead,” Science, vol. 362, no. 6412, 2018.
- [8] E. Knill, R. Laflamme, and G. J. Milburn, “A scheme for efficient quantum computation with linear optics,” Nature, vol. 409, no. 6816, pp. 46–52, 2001.
- [9] M. A. Nielsen, “Optical quantum computation using cluster states,” Physical Review Letters, vol. 93, p. 040503, 2004.

- [10] D. Gottesman and I. L. Chuang, “Demonstrating the viability of universal quantum computation using teleportation and single-qubit operations,” Nature, vol. 402, no. 6760, pp. 390–393, 1999.
- [11] H. Jeong and M. S. Kim, “Purification of entangled coherent states,” Quantum Information and Computation, vol. 2, no. 3, pp. 208–221, 2002.
- [12] Y.-B. Sheng, L. Zhou, and G.-L. Long, “Hybrid entanglement purification for quantum repeaters,” Physical Review A, vol. 88, p. 022302, Aug 2013.
- [13] M. Zukowski, A. Zeilinger, M. A. Horne, and A. K. Ekert, ““event-ready-detectors” bell experiment via entanglement swapping,” Physical Review Letters, vol. 71, pp. 4287–4290, Dec 1993.
- [14] W. J. Munro, A. M. Stephens, S. J. Devitt, K. A. Harrison, and K. Nemoto, “Quantum communication without the necessity of quantum memories,” Nature Photonics, vol. 6, pp. 777 EP –, 2012. Article.
- [15] S. Muralidharan, J. Kim, N. Lütkenhaus, M. D. Lukin, and L. Jiang, “Ultrafast and fault-tolerant quantum communication across long distances,” Physical Review Letters, vol. 112, p. 250501, Jun 2014.
- [16] F. Ewert and P. van Loock, “Ultrafast fault-tolerant long-distance quantum communication with static linear optics,” Physical Review A, vol. 95, p. 012327, Jan 2017.
- [17] S.-W. Lee, T. C. Ralph, and H. Jeong, “Fundamental building block for all-optical scalable quantum networks,” Physical Review A, vol. 100, p. 052303, Nov 2019.
- [18] T. Baumgratz, M. Cramer, and M. B. Plenio, “Quantifying coherence,” Physical Review Letters, vol. 113, p. 140401, Sep 2014.
- [19] R. Takagi and Q. Zhuang, “Convex resource theory of non-gaussianity,” Physical Review A, vol. 97, p. 062337, Jun 2018.

- [20] B. Yadin, F. C. Binder, J. Thompson, V. Narasimhachar, M. Gu, and M. S. Kim, “Operational resource theory of continuous-variable non-classicality,” Physical Review X, vol. 8, p. 041038, Dec 2018.
- [21] H. Kwon, K. C. Tan, T. Volkoff, and H. Jeong, “Nonclassicality as a quantifiable resource for quantum metrology,” Physical Review Letters, vol. 122, p. 040503, Feb 2019.
- [22] M. Fox, Quantum optics: an introduction. Oxford master series in atomic, optical, and laser physics, Oxford: Oxford Univ. Press, 2006.
- [23] J. L. Dodd, T. C. Ralph, and G. J. Milburn, “Experimental requirements for grover’s algorithm in optical quantum computation,” Physical Review A, vol. 68, p. 042328, Oct 2003.
- [24] H.-W. Lee and J. Kim, “Quantum teleportation and bell’s inequality using single-particle entanglement,” Physical Review A, vol. 63, p. 012305, Dec 2000.
- [25] A. P. Lund and T. C. Ralph, “Nondeterministic gates for photonic single-rail quantum logic,” Physical Review A, vol. 66, p. 032307, Sep 2002.
- [26] H. Jeong, M. S. Kim, and J. Lee, “Quantum-information processing for a coherent superposition state via a mixedentangled coherent channel,” Physical Review A, vol. 64, p. 052308, Oct 2001.
- [27] H. Jeong and M. S. Kim, “Purification of entangled coherent states,” Quantum Information and Computation, vol. 2, pp. 208–221, 2001.
- [28] N. Lütkenhaus, J. Calsamiglia, and K.-A. Suominen, “Bell measurements for teleportation,” Physical Review A, vol. 59, pp. 3295–3300, May 1999.
- [29] J. Calsamiglia and N. Lütkenhaus, “Maximum efficiency of a linear-optical bell-state analyzer,” Applied Physics B, vol. 72, no. 1, pp. 67–71, 2001.

- [30] S. J. D. Phoenix, “Wave-packet evolution in the damped oscillator,” Physical Review A, vol. 41, pp. 5132–5138, May 1990.
- [31] U. Leonhardt, “Quantum statistics of a lossless beam splitter: $Su(2)$ symmetry in phase space,” Physical Review A, vol. 48, pp. 3265–3277, Oct 1993.
- [32] H. Jeong, A. Zavatta, M. Kang, S.-W. Lee, L. S. Costanzo, S. Grandi, T. C. Ralph, and M. Bellini, “Generation of hybrid entanglement of light,” Nature Photonics, vol. 8, no. 7, pp. 564–569, 2014.
- [33] S.-W. Lee and H. Jeong, “Near-deterministic quantum teleportation and resource-efficient quantum computation using linear optics and hybrid qubits,” Physical Review A, vol. 87, p. 022326, Feb 2013.
- [34] S.-W. Lee, K. Park, T. C. Ralph, and H. Jeong, “Nearly deterministic bell measurement for multiphoton qubits and its application to quantum information processing,” Physical Review Letters, vol. 114, p. 113603, Mar 2015.
- [35] S.-W. Lee, K. Park, T. C. Ralph, and H. Jeong, “Nearly deterministic bell measurement with multiphoton entanglement for efficient quantum-information processing,” Physical Review A, vol. 92, p. 052324, Nov 2015.
- [36] G. Vidal and R. F. Werner, “Computable measure of entanglement,” Physical Review A, vol. 65, p. 032314, Feb 2002.
- [37] H. Jeong and M. S. Kim, “Efficient quantum computation using coherent states,” Physical Review A, vol. 65, p. 042305, Mar 2002.
- [38] T. C. Ralph, A. Gilchrist, G. J. Milburn, W. J. Munro, and S. Glancy, “Quantum computation with optical coherent states,” Physical Review A, vol. 68, p. 042319, Oct 2003.
- [39] K. Park, S.-W. Lee, and H. Jeong, “Quantum teleportation between particlelike and fieldlike qubits using hybrid entanglement under decoherence effects,” Physical Review A, vol. 86, p. 062301, Dec 2012.

- [40] S. Massar and S. Popescu, “Optimal extraction of information from finite quantum ensembles,” Physical Review Letters, vol. 74, pp. 1259–1263, Feb 1995.
- [41] A. P. Lund, T. C. Ralph, and H. L. Haselgrove, “Fault-tolerant linear optical quantum computing with small-amplitude coherent states,” Physical Review Letters, vol. 100, p. 030503, Jan 2008.
- [42] F. Fröwis, P. Sekatski, W. Dür, N. Gisin, and N. Sangouard, “Macroscopic quantum states: Measures, fragility, and implementations,” Reviews of Modern Physics, vol. 90, p. 025004, May 2018.
- [43] O. Morin, K. Huang, J. Liu, H. Le Jeannic, C. Fabre, and J. Laurat, “Remote creation of hybrid entanglement between particle-like and wave-like optical qubits,” Nature Photonics, vol. 8, no. 7, pp. 570–574, 2014.
- [44] D. E. Browne and T. Rudolph, “Resource-efficient linear optical quantum computation,” Physical Review Letters, vol. 95, p. 010501, Jun 2005.
- [45] M. Varnava, D. E. Browne, and T. Rudolph, “How good must single photon sources and detectors be for efficient linear optical quantum computation?,” Physical Review Letters, vol. 100, p. 060502, Feb 2008.
- [46] Y. Li, P. C. Humphreys, G. J. Mendoza, and S. C. Benjamin, “Resource costs for fault-tolerant linear optical quantum computing,” Physical Review X, vol. 5, p. 041007, Oct 2015.
- [47] N. K. Langford, S. Ramelow, R. Prevedel, W. J. Munro, G. J. Milburn, and A. Zeilinger, “Efficient quantum computing using coherent photon conversion,” Nature, vol. 478, no. 7369, pp. 360–363, 2011.
- [48] C. Zhang, Y.-F. Huang, C.-J. Zhang, J. Wang, B.-H. Liu, C.-F. Li, and G.-C. Guo, “Generation and applications of an ultrahigh-fidelity four-

photon greenberger-horne-zeilinger state,” Optics Express, vol. 24, pp. 27059–27069, Nov 2016.

- [49] C. Zhang, Y.-F. Huang, Z. Wang, B.-H. Liu, C.-F. Li, and G.-C. Guo, “Experimental greenberger-horne-zeilinger-type six-photon quantum nonlocality,” Physical Review Letters, vol. 115, p. 260402, Dec 2015.
- [50] Y.-F. Huang, B.-H. Liu, L. Peng, Y.-H. Li, L. Li, C.-F. Li, and G.-C. Guo, “Experimental generation of an eight-photon greenberger-horne-zeilinger state,” Nature Communications, vol. 2, pp. 546 EP –, 2011. Article.
- [51] X.-L. Wang, L.-K. Chen, W. Li, H.-L. Huang, C. Liu, C. Chen, Y.-H. Luo, Z.-E. Su, D. Wu, Z.-D. Li, H. Lu, Y. Hu, X. Jiang, C.-Z. Peng, L. Li, N.-L. Liu, Y.-A. Chen, C.-Y. Lu, and J.-W. Pan, “Experimental ten-photon entanglement,” Physical Review Letters, vol. 117, p. 210502, Nov 2016.
- [52] H.-S. Zhong, Y. Li, W. Li, L.-C. Peng, Z.-E. Su, Y. Hu, Y.-M. He, X. Ding, W. Zhang, H. Li, L. Zhang, Z. Wang, L. You, X.-L. Wang, X. Jiang, L. Li, Y.-A. Chen, N.-L. Liu, C.-Y. Lu, and J.-W. Pan, “12-photon entanglement and scalable scattershot boson sampling with optimal entangled-photon pairs from parametric down-conversion,” Physical Review Letters, vol. 121, p. 250505, Dec 2018.
- [53] D. R. Hamel, L. K. Shalm, H. Hübel, A. J. Miller, F. Marsili, V. B. Verma, R. P. Mirin, S. W. Nam, K. J. Resch, and T. Jennewein, “Direct generation of three-photon polarization entanglement,” Nature Photonics, vol. 8, pp. 801 EP –, 2014.
- [54] T. C. Ralph, A. P. Lund, and H. M. Wiseman, “Adaptive phase measurements in linear optical quantum computation,” J. Opt. B: Quantum Semiclass. Opt., vol. 7, pp. S245–S249, sep 2005.
- [55] J. Fiurášek, “Interconversion between single-rail and dual-rail photonic qubits,” Physical Review A, vol. 95, p. 033802, Mar 2017.

- [56] D. Drahı, D. V. Sychev, K. K. P., E. A. Sazhina, V. A. Novikov, I. A. Walmsley, and A. I. Lvovsky, “Quantum interface between single-and dual-rail optical qubits,” [arXiv:1905.08562](#), 2019.
- [57] H. Kwon and H. Jeong, “Generation of hybrid entanglement between a single-photon polarization qubit and a coherent state,” Physical Review A, vol. 91, p. 012340, Jan 2015.
- [58] D. V. Sychev, A. E. Ulanov, A. A. Pushkina, M. W. Richards, I. A. Fedorov, and A. I. Lvovsky, “Enlargement of optical schrödinger’s cat states,” Nature Photonics, vol. 11, no. 6, pp. 379–382, 2017.
- [59] J.-W. Pan, C. Simon, C. Brukner, and A. Zeilinger, “Entanglement purification for quantum communication,” Nature, vol. 410, no. 6832, pp. 1067–1070, 2001.
- [60] J.-W. Pan, S. Gasparoni, R. Ursin, G. Weihs, and A. Zeilinger, “Experimental entanglement purification of arbitrary unknown states,” Nature, vol. 423, no. 6938, pp. 417–422, 2003.
- [61] C. Simon and J.-W. Pan, “Polarization entanglement purification using spatial entanglement,” Physical Review Letters, vol. 89, p. 257901, Dec 2002.
- [62] C. Cai, L. Zhou, and S. Y.-B., “Fast multi-copy entanglement purification with linear optics,” Chinese Physics B, vol. 24, p. 120306, dec 2015.
- [63] Y.-B. Sheng, F.-G. Deng, and H.-Y. Zhou, “Efficient polarization-entanglement purification based on parametric down-conversion sources with cross-kerr nonlinearity,” Physical Review A, vol. 77, p. 042308, Apr 2008.
- [64] H. Zhang, Q. Liu, X.-S. Xu, J. Xiong, A. Alsaedi, T. Hayat, and F.-G. Deng, “Polarization entanglement purification of nonlocal microwave photons based on the cross-kerr effect in circuit qed,” Physical Review A, vol. 96, p. 052330, Nov 2017.

- [65] D. Salart, O. Landry, N. Sangouard, N. Gisin, H. Herrmann, B. Sanguinetti, C. Simon, W. Sohler, R. T. Thew, A. Thomas, and H. Zbinden, “Purification of single-photon entanglement,” Physical Review Letters, vol. 104, p. 180504, May 2010.
- [66] D. F. Walls and G. J. Milburn, “Effect of dissipation on quantum coherence,” Physical Review A, vol. 31, pp. 2403–2408, Apr 1985.
- [67] D. P. DiVincenzo and D. Loss, “Quantum computers and quantum coherence,” Journal of Magnetism and Magnetic Materials, vol. 200, no. 1, pp. 202 – 218, 1999.
- [68] W. H. Miller, “Perspective: Quantum or classical coherence?,” The Journal of Chemical Physics, vol. 136, no. 21, p. 210901, 2012.
- [69] K. C. Tan, H. Kwon, C.-Y. Park, and H. Jeong, “Unified view of quantum correlations and quantum coherence,” Physical Review A, vol. 94, p. 022329, Aug 2016.
- [70] A. Streltsov, U. Singh, H. S. Dhar, M. N. Bera, and G. Adesso, “Measuring quantum coherence with entanglement,” Physical Review Letters, vol. 115, p. 020403, Jul 2015.
- [71] J. Ma, B. Yadin, D. Girolami, V. Vedral, and M. Gu, “Converting coherence to quantum correlations,” Physical Review Letters, vol. 116, p. 160407, Apr 2016.
- [72] B. Yadin and V. Vedral, “Quantum macroscopicity versus distillation of macroscopic superpositions,” Physical Review A, vol. 92, p. 022356, Aug 2015.
- [73] H. Kwon, C.-Y. Park, K. C. Tan, and H. Jeong, “Disturbance-based measure of macroscopic coherence,” New Journal of Physics, vol. 19, p. 043024, apr 2017.
- [74] K. C. Tan, T. Volkoff, H. Kwon, and H. Jeong, “Quantifying the coherence between coherent states,” Physical Review Letters, vol. 119, p. 190405, Nov 2017.

- [75] Y.-R. Zhang, L.-H. Shao, Y. Li, and H. Fan, “Quantifying coherence in infinite-dimensional systems,” Physical Review A, vol. 93, p. 012334, Jan 2016.
- [76] J. Xu, “Quantifying coherence of gaussian states,” Physical Review A, vol. 93, p. 032111, Mar 2016.
- [77] Y.-T. Wang, J.-S. Tang, Z.-Y. Wei, S. Yu, Z.-J. Ke, X.-Y. Xu, C.-F. Li, and G.-C. Guo, “Directly measuring the degree of quantum coherence using interference fringes,” Physical Review Letters, vol. 118, p. 020403, Jan 2017.
- [78] P. Giorda and M. Allegra, “Coherence in quantum estimation,” Journal of Physics A: Mathematical and Theoretical, vol. 51, p. 025302, dec 2017.
- [79] M. Hillery, “Coherence as a resource in decision problems: The deutsch-jozsa algorithm and a variation,” Physical Review A, vol. 93, p. 012111, Jan 2016.
- [80] J. M. Matera, D. Egloff, N. Killoran, and M. B. Plenio, “Coherent control of quantum systems as a resource theory,” Quantum Science and Technology, vol. 1, p. 01LT01, aug 2016.
- [81] E. Schrödinger, “Der stetige übergang von der mikro- zur makromechanik,” Naturwissenschaften, vol. 14, no. 28, pp. 664–666, 1926.
- [82] R. J. Glauber, “Coherent and incoherent states of the radiation field,” Physical Review, vol. 131, pp. 2766–2788, 1963.
- [83] E. C. G. Sudarshan, “Equivalence of semiclassical and quantum mechanical descriptions of statistical light beams,” Physical Review Letters, vol. 10, pp. 277–279, 1963.
- [84] C. M. Caves, “Quantum-mechanical noise in an interferometer,” Phys. Rev. D, vol. 23, pp. 1693–1708, Apr 1981.

- [85] A. Furusawa, J. L. Sørensen, S. L. Braunstein, C. A. Fuchs, H. J. Kimble, and E. S. Polzik, “Unconditional quantum teleportation,” Science, vol. 282, no. 5389, pp. 706–709, 1998.
- [86] M. Hillery, “Quantum cryptography with squeezed states,” Physical Review A, vol. 61, p. 022309, Jan 2000.
- [87] S. L. Braunstein and P. van Loock, “Quantum information with continuous variables,” Reviews of Modern Physics, vol. 77, pp. 513–577, Jun 2005.
- [88] S. D. Bartlett and B. C. Sanders, “Requirement for quantum computation,” Journal of Modern Optics, vol. 50, no. 15-17, pp. 2331–2340, 2003.
- [89] K. Kraus, States, Effects and Operations: Fundamental Notions of Quantum Theory. Springer, Berlin, 1983.
- [90] M.-D. Choi, “Completely positive linear maps on complex matrices,” Linear Algebra and its Applications, vol. 10, no. 3, pp. 285 – 290, 1975.
- [91] A. Jamiołkowski, “Linear transformations which preserve trace and positive semidefiniteness of operators,” Reports on Mathematical Physics, vol. 3, no. 4, pp. 275 – 278, 1972.
- [92] J. Aberg, “Quantifying superposition,” arXiv:quant-ph/0612146, 2006.
- [93] A. Streltsov, G. Adesso, and M. B. Plenio, “Colloquium: Quantum coherence as a resource,” Reviews of Modern Physics, vol. 89, p. 041003, Oct 2017.
- [94] X. Yuan, H. Zhou, Z. Cao, and X. Ma, “Intrinsic randomness as a measure of quantum coherence,” Physical Review A, vol. 92, p. 022124, Aug 2015.

- [95] A. Winter and D. Yang, “Operational resource theory of coherence,” Physical Review Letters, vol. 116, p. 120404, Mar 2016.
- [96] K. C. Tan, S. Choi, H. Kwon, and H. Jeong, “Coherence, quantum fisher information, superradiance, and entanglement as interconvertible resources,” Physical Review A, vol. 97, p. 052304, May 2018.
- [97] T. Durt, B.-G. Englert, I. Bengtsson, and K. Życzkowski, “On mutually unbiased bases,” International Journal of Quantum Information, vol. 08, no. 04, pp. 535–640, 2010.
- [98] C. Napoli, T. R. Bromley, M. Cianciaruso, M. Piani, N. Johnston, and G. Adesso, “Robustness of coherence: An operational and observable measure of quantum coherence,” Physical Review Letters, vol. 116, p. 150502, Apr 2016.
- [99] M. Piani, M. Cianciaruso, T. R. Bromley, C. Napoli, N. Johnston, and G. Adesso, “Robustness of asymmetry and coherence of quantum states,” Physical Review A, vol. 93, p. 042107, Apr 2016.
- [100] B. Regula, K. Fang, X. Wang, and G. Adesso, “One-shot coherence distillation,” Physical Review Letters, vol. 121, p. 010401, Jul 2018.
- [101] K. Fang, X. Wang, L. Lami, B. Regula, and G. Adesso, “Probabilistic distillation of quantum coherence,” Physical Review Letters, vol. 121, p. 070404, Aug 2018.
- [102] M. G. Díaz, K. Fang, X. Wang, M. Rosati, M. Skotiniotis, J. Calsamiglia, and A. Winter, “Using and reusing coherence to realize quantum processes,” Quantum, vol. 2, p. 100, Oct. 2018.
- [103] K. Bu, N. Anand, and U. Singh, “Asymmetry and coherence weight of quantum states,” Physical Review A, vol. 97, p. 032342, Mar 2018.
- [104] S. Du, Z. Bai, and Y. Guo, “Conditions for coherence transformations under incoherent operations,” Physical Review A, vol. 91, p. 052120, May 2015.

- [105] T. Kiesel and W. Vogel, “Nonclassicality filters and quasiprobabilities,” Physical Review A, vol. 82, p. 032107, Sep 2010.
- [106] G. Vidal and R. Tarrach, “Robustness of entanglement,” Physical Review A, vol. 59, pp. 141–155, Jan 1999.
- [107] K. C. Tan and H. Jeong, “Nonclassical light and metrological power: An introductory review,” AVS Quantum Science, vol. 1, no. 1, p. 014701, 2019.
- [108] C. T. Lee, “Measure of the nonclassicality of nonclassical states,” Physical Review A, vol. 44, pp. R2775–R2778, Sep 1991.
- [109] B. Kühn and W. Vogel, “Preparation of arbitrary quantum states with regular p functions,” Physical Review A, vol. 98, p. 053807, Nov 2018.
- [110] H. Pashayan, J. J. Wallman, and S. D. Bartlett, “Estimating outcome probabilities of quantum circuits using quasiprobabilities,” Physical Review Letters, vol. 115, p. 070501, Aug 2015.
- [111] T. Kiesel, W. Vogel, V. Parigi, A. Zavatta, and M. Bellini, “Experimental determination of a nonclassical glauher-sudarshan p function,” Physical Review A, vol. 78, p. 021804, Aug 2008.
- [112] I. Marvian and R. W. Spekkens, “How to quantify coherence: Distinguishing speakable and unspeakable notions,” Physical Review A, vol. 94, p. 052324, Nov 2016.
- [113] W. Zheng, Z. Ma, H. Wang, S.-M. Fei, and X. Peng, “Experimental demonstration of observability and operability of robustness of coherence,” Physical Review Letters, vol. 120, p. 230504, Jun 2018.
- [114] K. C. Tan, S. Choi, and H. Jeong, “Negativity of quasiprobability distributions as a measure of nonclassicality,” Physical Review Letters, vol. 124, p. 110404, Mar 2020.

- [115] H. Kim, J. Park, and H. Jeong, “Transfer of different types of optical qubits over a lossy environment,” Physical Review A, vol. 89, p. 042303, Apr 2014.

국문초록

광학 시스템은 양자 정보 처리에서 유망한 후보 중 하나이며 양자 자원을 활용하여 양자적 이점을 얻을 수 있는 많은 응용이 존재한다. 양자 텔레포테이션은 잘 알려진 프로토콜 중 하나로서 양자 얽힘을 이용한다. 그러나 광자 손실은 양자 얽힘에 불가피하게 손상을 주고, 이는 많은 광자로 구성된 큐빗의 경우 더 심각한 영향을 끼친다.

이 논문은 서로 다른 두 종류의 큐빗 인코딩 사이의 얽힘을 이용하는 이중 양자 얽힘을 사용하고 높은 텔레포테이션 성공 확률과 순결성을 동시에 달성하는 방법에 대해 논의한다. 높은 성공 확률을 위해 이 논문에서는 거의 확정적인 벨 측정을 수행할 수 있는 큰 진폭의 결맞음 큐빗과 편광된 광자로 구성된 다광자 큐빗을 고려한다. 한편, 적은 광자를 가진 큐빗들은 광자 손실에 의한 영향이 상대적으로 적다. 이러한 큐빗의 후보로 진공-단일 광자 큐빗, 편광된 단일 광자 큐빗, 작은 진폭의 결맞음 큐빗이 고려된다. 큰 진폭의 결맞음 큐빗은 진공-단일 광자 큐빗과 이중 얽힘을, 그리고 다광자 큐빗은 세가지의 작은 광자 큐비트에 대한 얽힘을 고려한다.

먼저, 큰 진폭의 결맞음 큐빗을 이용한 이중 양자 얽힘에 대한 분석은 큐빗의 진폭이 클수록 성공 확률이 더 많은 광자 손실에 대해서도 높게 유지된다는 것이 나타난다. 순결성은 결맞음 큐빗과 진공-단일 광자 큐빗 모두의 손실에 영향을 받지만, 진폭이 클수록 결맞음 큐빗의 손실에 대한 영향을 더 크게 받는 것을 볼 수 있다. 둘째로, 다광자 큐빗의 이중 양자 얽힘에서는 순결성이 작은 광자 큐빗에서 일어나는 손실에만 영향을 받는 반면 성공 확률은 다광자 큐빗의 손실에만 영향 받음을 보인다. 특히 높은

순결성 영역에서 ($F \geq 90\%$) 진공-단일 광자 큐빗은 다광자 큐빗을 직접 전송하는 방법 보다 10배 많은 광자 손실률을 견딘다는 것을 보인다. 성공 확률에 대해, 이 논문은 주어진 손실률에 대해 다광자 큐빗의 최적의 광자 수 또한 제시한다. 추가적으로 이중 양자 얽힘을 생성할 수 있는 실험적 방법이 논의된다.

여기에 더 나아가 양자 얽힘 외에 빛이 가질 수 있는 양자 자원인 양자 결맞음과 비고전성을 자원 이론 관점에서 다룬다. 먼저 결맞음 이론에 대해 양자 측도 세기와 양자 관측량의 평균값이라는 물리적인 현상에 기초한 측도를 제시한다. 후자의 경우 양행렬 프로그래밍을 통해 필요한 최적화 계산을 수행 할 수 있음을 보인다. 이 논문에서 제시된 비고전성의 측도는 글라우버-수다르산 P -함수의 음수성에 기초하며, P -함수의 특이점을 필터링을 통해 푸리에 공간에서 다룬다. 이러한 음수성은 고전 상태와 혼합을 견디는 정도와 같다는 것을 증명하여, 조작적인 관점에서 의미 또한 제시한다.

주요어 : 양자 공간 이동, 이중 양자 얽힘, 양자 결맞음, 비고전성

학번 : 2015-20354

감사의 글

먼저, 저를 지금까지 인도해 주셨고 그리고 앞으로도 그러하실 하나님께 감사드립니다.

대학원에 들어와서 많은 분들께 참 많은 도움을 받았습니다. 정현석 교수님께 부족함이 많은 저를 제자로 삼으시고 5년이 넘는 학위 기간동안 지도해 주시고 많은 도움을 주신 것에 대해 감사드리고 싶습니다. 바쁘신 가운데 심사를 맡아 주신 안경원 교수님, 김석 교수님, 박철환 교수님, 이승우 교수님께 감사드립니다.

연구실 생활에서 힘이 되어 주시고 학술적으로나 그 외적인 부분에서나 많은 것들을 배울 수 있었던 임영룡, 양승호, 김호용, 박채연, 권혁준, 안대건, 오창훈, 전인우 선배님들과 Yong Siah Teo, Omkar Srikrishna 박사님, 연구에서 많은 도움을 주신 Tan Kok Chuan Bobby 박사님께 감사합니다. 또한, 가르쳐줄 것 보다 배우는 것이 더 많았던 Lie석형, Lee석형, 신성욱, 권혁건 후배들에게도 감사의 말을 전합니다. 이 분들 덕분에 짧지 않은 학위 과정이 즐거웠던 추억으로 기억될 수 있었습니다.

그리고 박사 학위 동안 저를 지지해준 가족, 친지 분들께 심심한 감사를 드리고 싶습니다. 특히, 신앙의 바른 길을 보여주신 부모님, 긴 학위 기간동안 저를 믿어주신 처부모님께 다시 한 번 감사드립니다. 마지막으로 이 학위 기간을 시작하며 만나 저를 아껴주고 응원하여 주었던 사랑하는 아내 세진이에게도 감사를 전하고자 합니다.